IMPROVED RESERVOIR CHARACTERIZATION OF PAB SANDSTONE BY INTEGRATING PETROPHYSICS, SEISMIC INVERSION, AND ROCK PHYSICAL ANALYSIS OF ZAMZAMA GAS FIELD, LOWER INDUS BASIN, PAKISTAN.

BY

ABDUL MAJEED

M.PHIL GEOPHYSICS

2020-2022

DEPARTMENT OF EARTH SCIENCE

QUAID-I-AZAM UNIVERSITY

ISLAMABAD, PAKISTAN

CERTIFICATE

This dissertation is submitted by **ABDUL MAJEED** S/O **MIRZA KHAN** is accepted in its present form by the Department of Earth Sciences as sustaining the requirement for the award of M.Phil degree in **Geophysics.**

RECOMMENDED BY

Dr. Tahir Azeem _____

(Supervisor)

Dr. Aamir Ali _____

(Chairman Department of Earth Sciences)

External Examinar _____

ACKNOWLEDGEMENT

In the name of the most forgiving and good-willed Allah. All praise to the All-Powerful, the One, the Everlasting, Who has no descendants, is inherited by no one, and has no equal. Alhamdulillah. I swear that the Holy Prophet Muhammad (PBUH) is the final messenger, whose life serves as an ideal example for the entirety of humanity up until the Day of Judgment. I thank Allah for giving me the courage and favour to complete my thesis.

Without your assistance, I am nothing. Please keep me always in prostration before you and let me not leave before anyone except you.

Foremost, I would like to express my sincere gratitude for my supervisor, **Dr. Tahir Azeem**, for his unwavering support during my M.Phil studies and research as well as for his inspiration, passion, vast knowledge, and faith in me. His wisdom was very instructive to me. His advice was helpful to me throughout the entire research and thesis-writing process. I couldn't have asked for a better mentor and advisor for my studies.

I am very grateful to all my teachers for their unending support, prayers, and encouragement. I also want to express my sincere gratitude to everybody who helped this research indirectly.

ABDUL MAJEED

Dedication

I would like to dedicate this research to my parents, whose love, support, and prayers throughout the day and night have enabled me to achieve such accomplishment and distinctions along with all the dedicated and well-liked teachers.

Abstract

Seismic reflection is an indirect geophysical technique that is frequently employed for oil exploration. The evaluation of the hydrocarbon reservoir and the characterization of the physical reservoir parameters are the main goals. Zamzama gas field is located in the Lower Indus Basin, which is under the influence of compressional regime. The Pab Formation of Late Cretaceous age which is composed of major sandstone but minor mudstone and shale components.

Due to thin layering of shale beds it is not characterized by conventional method. Using borehole data of Zamzama 03 reservoir zone is identified by petrophysical analysis. According to petrophysical data, the Pab Formation has a reasonable effective porosity of 10%, a small amount of shale of 21%, and a hydrocarbon saturation of 70–80.

For wells Zamzma-03, Rock Physics confirms the results of Petrophysical study and calculates reservoir rock physics parameters to obtain a good knowledge of reservoir attributes. As the Acoustic Impedance and Vp/Vs ratio decrease, it indicates the existence of reservoir zone. From facies analysis the cross plots of Acoustic Impedance and Vp/Vs ratio is plotted, a decrease in P-impedance and Vp/Vs ratio indicated a large amount of sands. Brine sand appears as a second type of sand in the cross plots due to its high Acoustic Impedance and Vp/Vs ratio. Presence of shale shows in cross plots but these values different from the earlier situation for both sand types, Shale can be found where the P-impedance is low but the Vp/Vs ratio is high.

Seismic interpretation is performed to delineate the subsurface structure. On a Synthetic Seismogram, Pab and Fort Munro are two horizons that are marked. Two faults are marked by distortions or discontinuities with an easterly-verging N-S thrust fault. Time and depth contour maps also validates subsurface structures.

The reservoir zone is confirmed by performing three types of post stack inversions. Model based (MBI) inversion, Sparse Spike Inversion (SSI), and band-limited inversion (BLI) are performed on seismic data. MBI has a correlation coefficient of 0.99 and a reservoir-level error of 0.05. SSI's correlation coefficient is (0.97) and its error is (0.024), while BLI's correlation coefficient is (0.97) and it likewise falls within acceptable ranges (0.90). All inversion results provide good results at reservoir level, but MBI performs the best followed by SSI and BLI.

Table of Contents

List of Figures

List of Tables

CHAPTER#1

INTRODUCTION TO DISSERTATION

1.1. Introduction

This dissertation uses 3D seismic interpretation and Seismic Inversion (SI) techniques to better comprehend the geophysical and geological characteristics of the Zamzama block in relation to hydrocarbon exploration and production. The Zamzama Block is around 200 kilometers north of Karachi in Pakistan's Sindh Province. This field is 129 kilometers long and 129 kilometers wide. It's a BHP Petroleum concession block that was found in 2007.

1.2. Research overview

Exploration geophysicists began working on the seismic approach in 1915, and it has since shown to be quite beneficial for imaging subsurface geological features and locating structural or stratigraphic traps (Coffeen, 1986). Seismic surveys, which display data as a time series of reflections across the subsurface, are commonly used in hydrocarbon exploration.

Since 1920, the seismic reflection technique has played an important role in exploration. The seismic technique is a key remote sensing technology for imaging subsurface strata at depths ranging from a few metres to kilometers. By source, the simple idea is to create an acoustic wave. This wave travels into the earth's subsurface, where it partially refracts and reflects due to lithological differences in Acoustic Impedance. The set of localized receivers on the surface records refracted and reflected seismic waves (Bakker, 2002).

The primary tool for hydrocarbon exploration is 3D seismic interpretation. It is carried out on the seismic cube of a gas field with sand reservoirs. 3D seismic surveys offer numerous benefits and can be used for a wide range of concerns, from exploration to development. They're also useful for limiting the scope of extensive reservoir characterization. The fundamental concept is to represent the subsurface structure as a simple model with resolvable parameters. In less disturbed places, seismic interpretation is usually a quick process, but in geologically complex locations, such as zones of low impedance, it can be slow and cautious. Then, based on this, contour maps of overlying sand reservoirs are created.

The study of rock characteristics and their interaction with fluids is known as petrophysical analysis. The most significant attribute of fluid for its storage and movement with in rock is porosity and permeability. Petrophysical logs provide most of data so they are employed in the mapping and identification of lithologies (George, 1982). The deposition environment

influences mineralogical properties of rock such as sorting, compaction, cementation, and grain size (Donaldson, 2015).

Seismic inversion is the primary tool used by geophysicists to better understand the subsurface. The information from well logs is extended to seismic volume through inversion. Different types of seismic inversion are employed to solve different challenges (Barclay et al. 2007). Seismic inversion is used to recover rock physical attributes from seismic data and provides a thorough image of subsurface geology. It is used to resolve seismic data and characterize reservoirs at various levels (Rajput & Ring, 2014).

Inversion is a technique for predicting, calculating, and inferring physical properties from real-world data (Sen., 2006). This resulted in more accurate estimates of reservoir parameters like as porosity, water saturation, volumetric, and so on. Another feature of inversion is the estimation of risks and uncertainties. As a result, the various inversion techniques can be useful in reservoir management and development.

1.3. Introduction to study area

Pakistan's southern and northern regions have a lot of hydrocarbon potential. The Lower Indus Basin has served as a possible zone for recovering a significant amount of hydrocarbon. The Zamzama gas field is located 200 kilometers north of Karachi in the Sindh region of Pakistan's Kirthar Fold Belt. The Zamzama gas field is shown in Figure 1.1. It has a surface area of 120 square kilometers and is Pakistan's fourth discovered gas deposit (Jackson et al., 2007). It's the eastward progressing thrusted anticline with a huge north-south oriented fault.

In the Kirthar Fold Belt, the late Cretaceous Pab Sandstone serves as a primary reservoir, while in the Zamzama gas field, it serves as the main reservoir. Bhit (southwest of Zamzama) and Kadanwari, Sawan, and Miano fields (northeast of Zamzama) are two other gas fields nearby.

The entire known recoverable reserves from the core area of the Zamzama field are estimated to be 1.7 Tcf of gas (Jackson et al., 2007). For the next 10 to 12 years, the field will produce roughly 320mmcf/d of gas and 2000 standard barrels of condensate (stb/d), with an economic field life of 15 to 25 years. The Zamzama gas is dry and sweet, with a condensate value to gas ratio of 6.5 barrels per million cubic feet (Jackson et al., 2007).

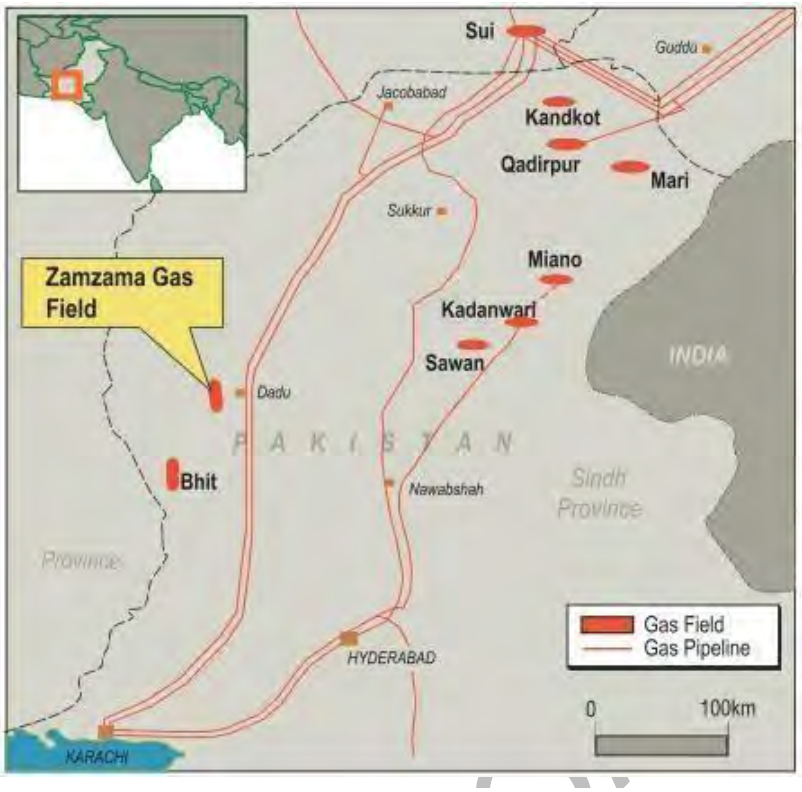

Figure 1.1:Major detection in Southern Indus Basin consist of gas field (Bhp billiton, 2003).

1.4. Geographical Boundaries

The Zamzama field is surrounded by the Kirthar range in the west, which consists of a 560 km long and 130-220 km wide belt with an NS direction, containing basins and valleys, while Sukkur is in the NE and district Hyderabad is in the SE, the river Indus is in the east, and Karachi is in the south. These boundaries are shown in figure 1.2.

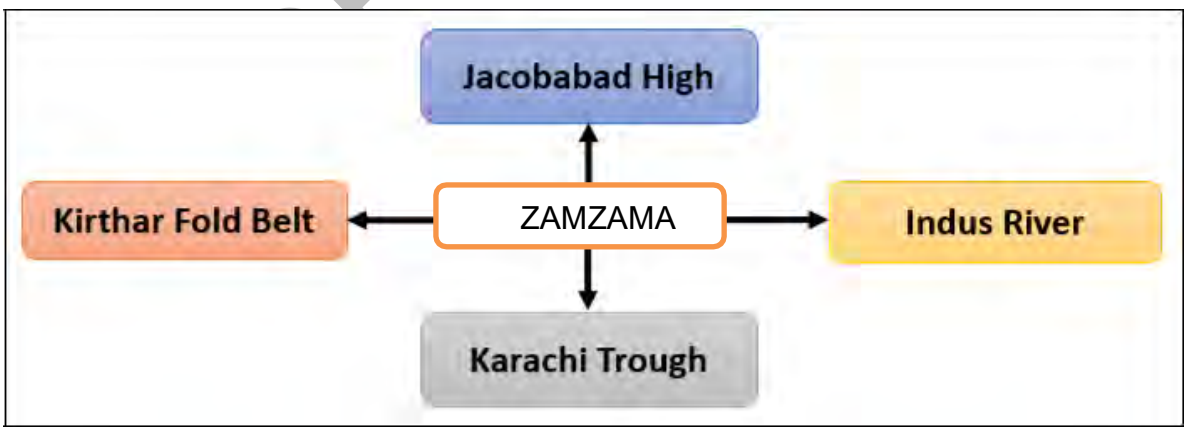

Figure 1.2: Geographical boundaries of Zamzama Gas Field.

1.5. Data Description

The data base is crucial to the project's success. The data is used in this study area to estimate the study goal, such as 3D seismic interpretation, petrophysics, and inversion. After gaining

approval from the DGPC(Directorate General of Petroleum Concessions)., the data was obtained from the LMKR with permission from the Department of Earth Science at Quaid-i-Azam University Islamabad. The description of seismic data and well data is shown in table 1.1 and 1.2 respectively. In seismic data inline starts from 411 to 516 and crossline starts from 1319 to 1447. Data from wells is presented in las format. There are three wells in the data set Zamzama-02, Zamzama-03, and Zamzama-05. Kingdom Software (IHS) is used to input 3D seismic data, and a base map is created. The base map depicts well locations, concern borders, seismic survey line direction, and survey shot positions as shown in figure 1.3. The geographic reference on the base maps that contain the cultural data of roads and buildings is latitude and longitude, or Universal Transverse Mercator (UTM) grid information. The base map depicts the locations of all inline, crosslines, and wells. Inline lines vary along the x-axis, while cross lines vary along the y-axis. The base map in geophysics shows the alignment of seismic lines and the locations where seismic data was collected (Sroor, 2010).

Table 1.1:Shows In-lines and Cross-lines information.

Lines	Start	End	Total In-lines & Cross-lines
In-line	411	516	105
Cross-line	1319	1447	128

Table 1.2:Wells Information of Zamzama Gas field.

Sr.no	**Well name**	**Latitude**	**Longitude**	**Total depth**	**Well type**	**Final Status**
1	Zamzama-02	26.6755	67.6545	4032	Appraisal	Suspended
2	Zamzama-03	26.7138	67.6682	3698	Development	Gas
3	Zamzama-05	26.6676	67.6706	3871	Development	Gas

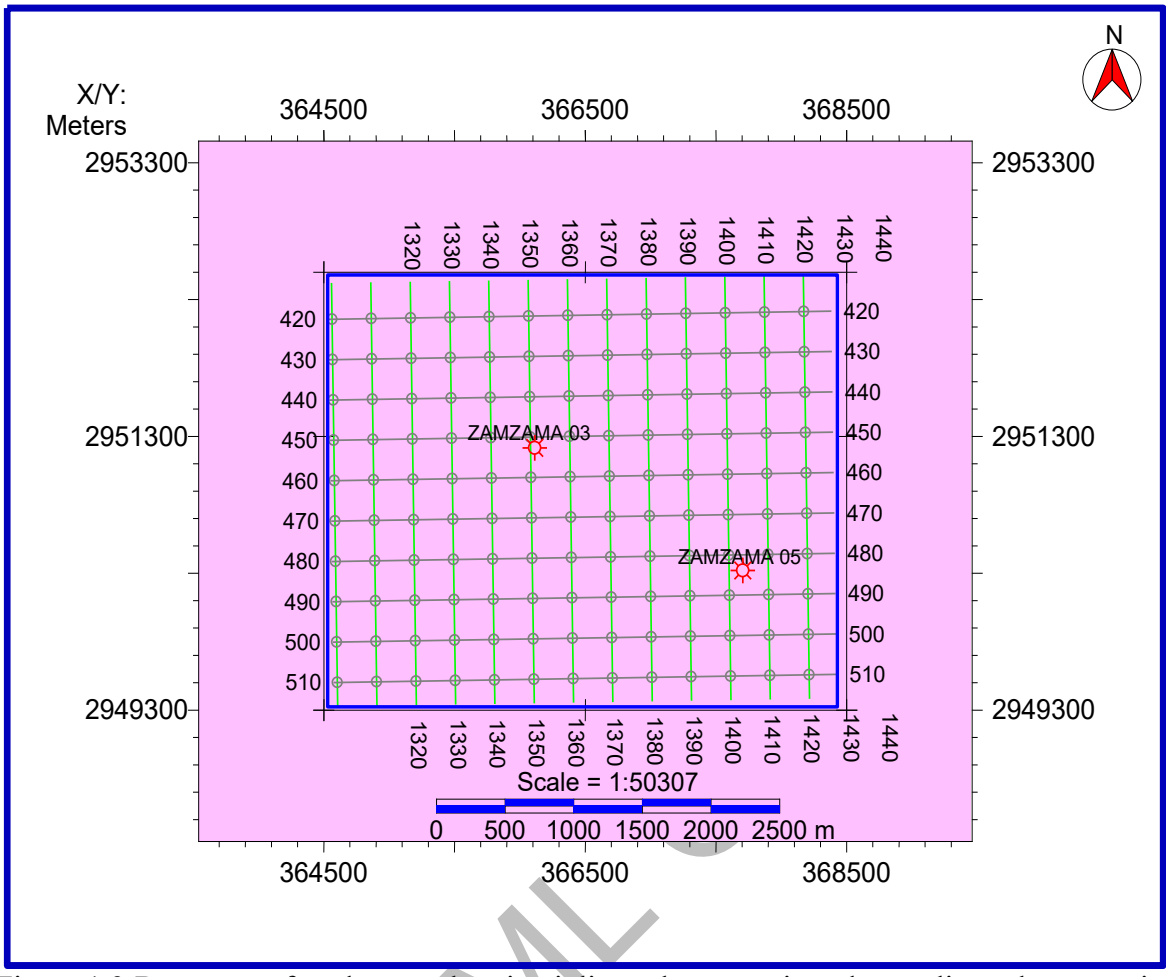

Figure 1.3:Base map of study area showing inlines along x-axis and cross lines along y-axis.

.

1.6. Objectives

The study area's key goals are as follows:

1) To delineate hydrocarbon potential zones using petrophysical analysis, Rock physical analysis/facies analysis of well log data.

2) Identification of suitable structures for hydrocarbon accumulation with the help of 3D seismic data interpretation.

3) To explore the lateral variation of Acoustic Impedance at reservoir level using seismic poststack inversion.

1.7. Workflow of research area

The workflow of research is shown in Figure 1.4. . Kingdom Software (IHS) is used to input 3D seismic data and well data. Well data is used to generate Synthetic Seismogram and petrophysical analysis. Synthetic Seismogram is then tied to seismic data for further seismic interpretation. Horizons are marked on seismic section and contours are generated for seismic section. Finally post stack inversion is applied to identify hydrocarbon potential zones.

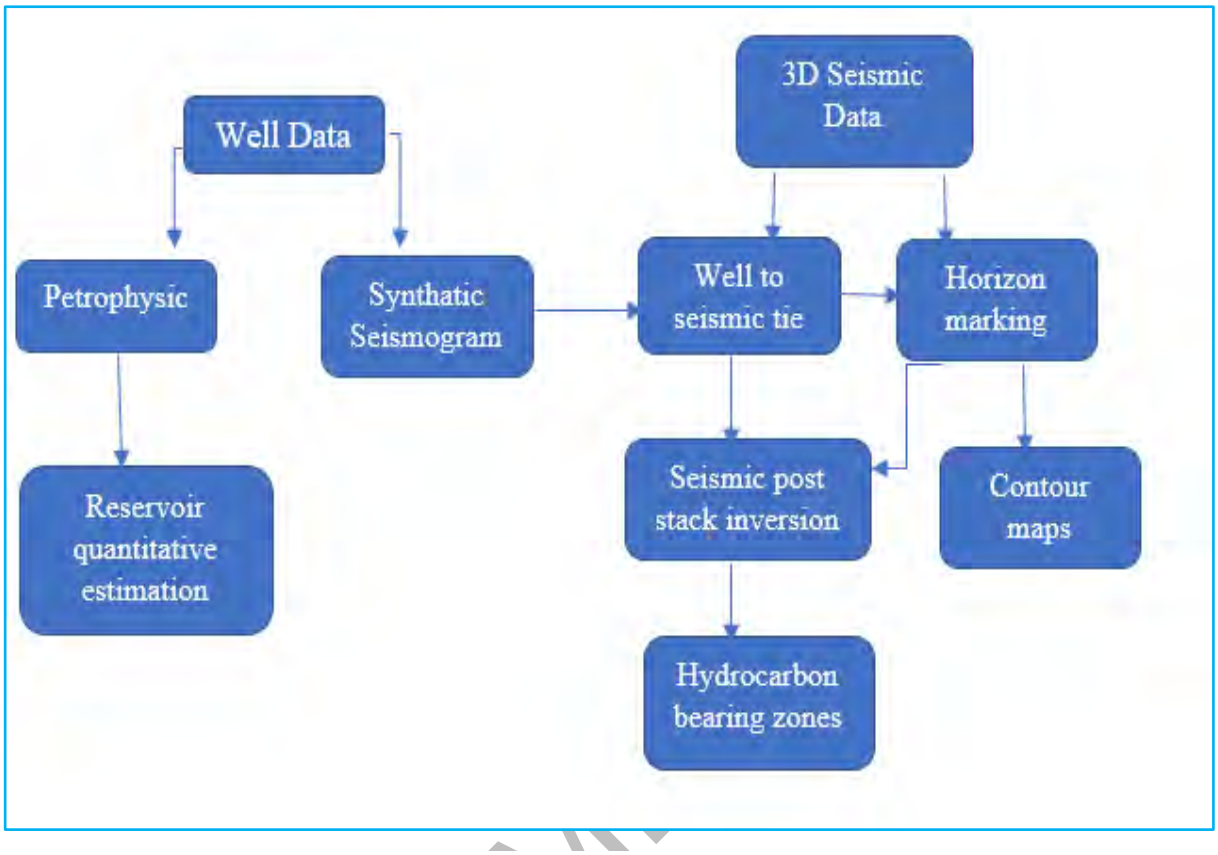

Figure 1.4:Workflow for seismic interpretation of study area.

CHAPTER#2

REGIONAL GEOLOGY AND TECTONICS

2.1. Introduction

The geology of the research area is crucial for seismic and stratigraphic interpretation (Bacon, Simm, & Redshaw, 2003). For proper seismic interpretation, geophysicists must be familiar with local and regional geology (Badley,1991).

The Zamzama block lies in the Kirthar Sub Basin, which is a sub-basin of the Southern Indus Basin, which is a sub-basin of the Lower Indus Basin, which is a sub-basin of the Indus Basin. The Zamzama block's geographical and Basinal location, petroleum history, tectonic, geological setting, depositional environment, structural style, stratigraphy, and petroleum system are all studied in detail.

2.2. Location

The Dadu area of Pakistan's Sindh province contains the Zamzama field, which is located 200 kilometers from Karachi. Indus River in the east and Karachi in the south, Kirthar Mountain ranges in the west, Sukker Mountain range in the north-east, Manchor Lake in the south, and Kirhter Mountain ranges in the east surrounds it. The Zamzama Block is about 130 and 120 kilometers wide and 560 kilometers long. The research area is shown in Figure 2.1, and it is situated in the centre and southern Kirthar Fold Belt.

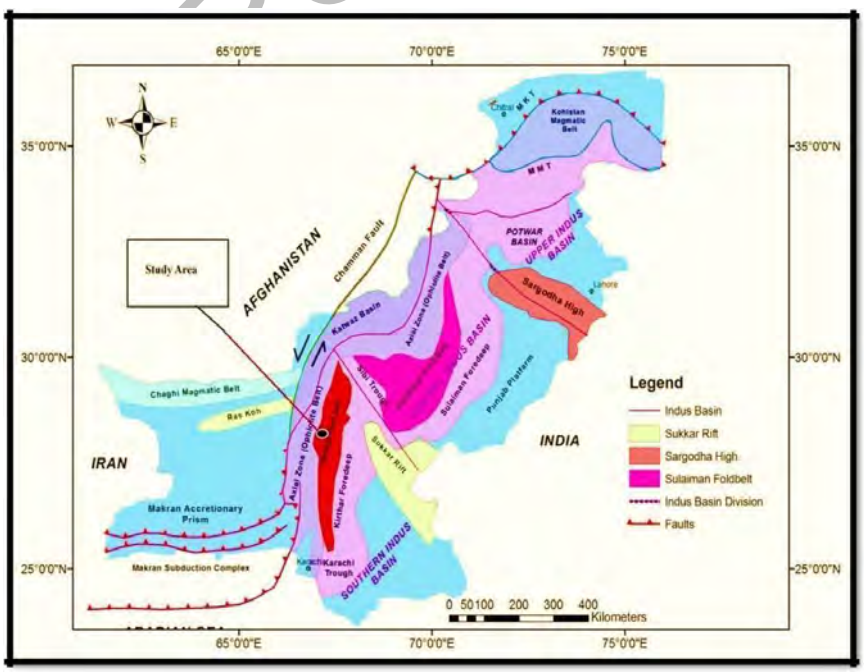

Figure 2.1: Location of Zamzama Block (Kadri, 1995)

2.2.1. Southern Indus Basin

The Zamzama Block is located in the Kirthar Subbasin, which is part of the Southern Indus Basin. It is located to the south of the Sukkur Rift. The Southern and Central Indus Basins are separated by the Sukkur Rift. The Indian shield to the east and the marginal zone of the Indian Plate to the west define the boundaries of the Southern Indus Basin. Its southern extension is bounded by the Murray Ridge off the coast (Kadri, 1995). Figure 2.2 depicts the Southern Indus, which is categorised as follows:

1.Thar Platform
2.Karachi Trough
3.Kirthar Foldbelt
4. Offshore Indus
5. Kirthar Foredeep

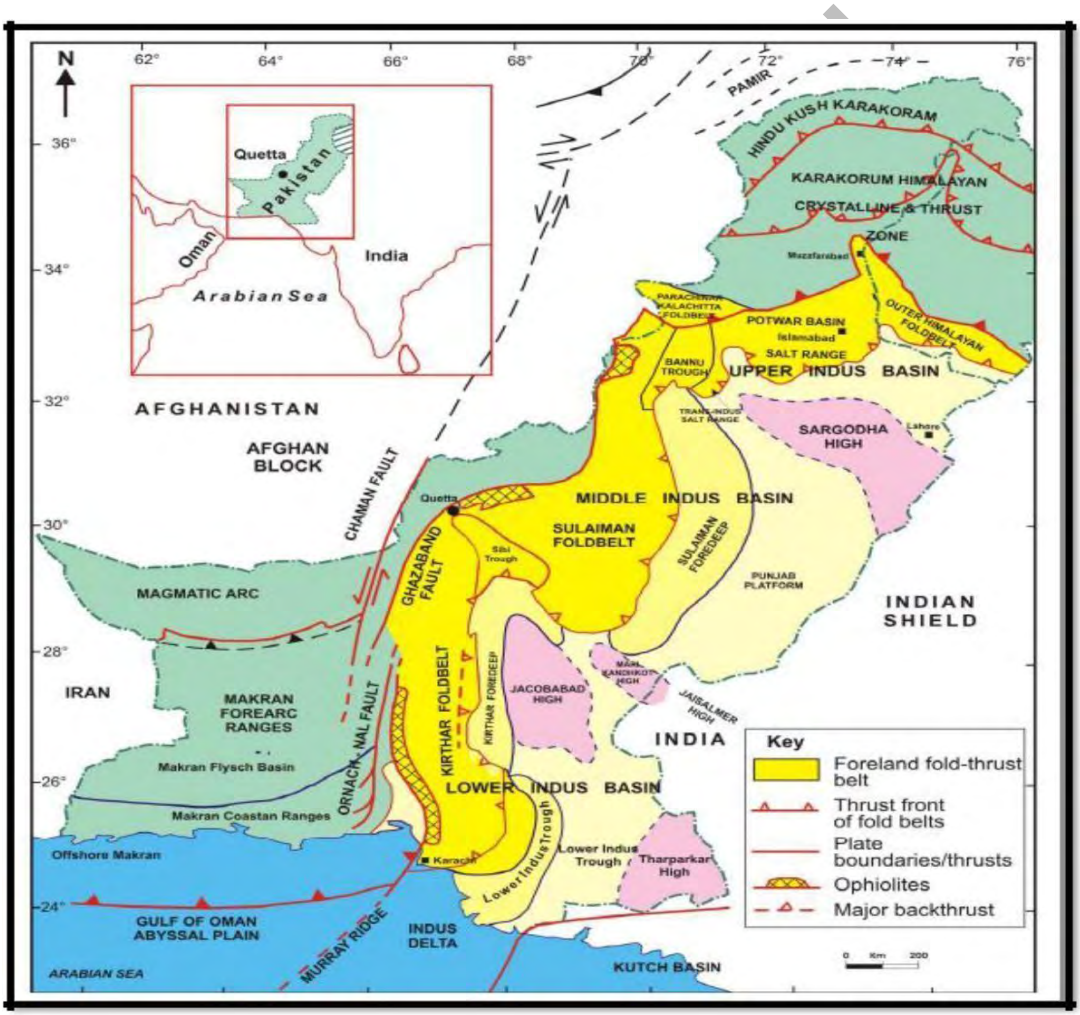

Figure 2.2: Southern Indus Basin (Kazmi and Jan, 1997).

2.2.2. Kirthar Sub Basin

The Zamzama Block is in the Kirthar Subbasin, which is part of the Southern Indus Basin and is part of the Kirthar Foldbelt. The Kirthar Sub Basin is depicted in above figure

2.2, which depicts Pakistan's Basinal categorization as well as the Southern Indus Basin's sub classification. The Indus Basin's Kirthar Fold Belt is a tectonic-stratigraphic province. The Kirther sub basin is a section of the Indus extracontinental trough down warp basin that formed on the Indian Plate (Raza, 2002). The Kirther Fold Belt, a North-South extended tectonic structure is structurally and stratigraphically comparable to the Sulaiman Fold Belt, is the subject of inquiry.

The Kirther Fold Belt is located along the western edge of the Indus Basin, which is connected to the Baluchistan Basin. The succession was deposited on the Indian Plate's northwestern passive border, which has been separated into the Sulaiman and Kirther blocks based on satellite pictures of its structural character (Bender and Raza, 1995).

The Kirthar Fold Belt was formed when the Indian Plate clashed with the Eurasian Plate during the collision phase. It is made up of a continuous series of fold-thrust belts (Bender and Raza, 1995). The belt stretches 350 kilometers and runs primarily north–south (Kazmi and Jan, 1997). The biggest mountain-building episode is thought to have occurred in the late 1800s. Pliocene–Pleistocene.

2.3. Petroleum History

The first exploration well at Zamzama, Zamzama-1/ST1, was spudded in January 1998. Extended test wells (ETW) were drilled in 2001, and full production began in the middle of 2003. The well, which was drilled to a total depth of 3,938 metres, discovered hydrocarbons in the Khadro and Pab Sandstones, and wireline logs verified a gas column of more than 300 metres. 3-D seismic acquisition and the drilling of the Zamzama-2 appraisal well were part of the appraisal program. The Zamzama-2 well was sunk to a depth of 3,933 metres and found hydrocarbons in the Khadro and Pab Sandstone formations. Zamzama -03, 04, and 05 were also drilled as development wells. This field is a large source of gas, ranking fourth in the country in terms of gas output with a low condensate to gas ratio of 6.5 barrels/MMcf, the gas is sweet and dry. The Zamzama gas field's anticipated production life is 15 to 25 years.

2.4. Structural Pattern

Open and symmetrical folds dominate the Kirthar Fold Belt, which are generated by inversion of basement-involved Jurassic extensional faults. Thrusts in the Eocene mudstones and thrusts with a deeper detachment in the Lower Cretaceous source rock interval that involve the reservoir during deformation defined by horst and Graben structures, as well as a system of transcrurrent faults, have been interpreted with two

detachments. (Zaigham & Mallick, 2000). A considerable number of anticlinal structures were formed on the eastern side of the Kirther Fold Belt as a result of plate collision during the Oligocene–Miocene period.

The research reveals Zamzama's structural style and evolution. Block that the predicted shortening along the Zamzama structure in figure (2.3) represents deformation akin to fault propagation folds. This indicates that a decollment exists beneath the building, resulting in Zamzama being a thin-skinned structure with no basement involvement in the deformation.

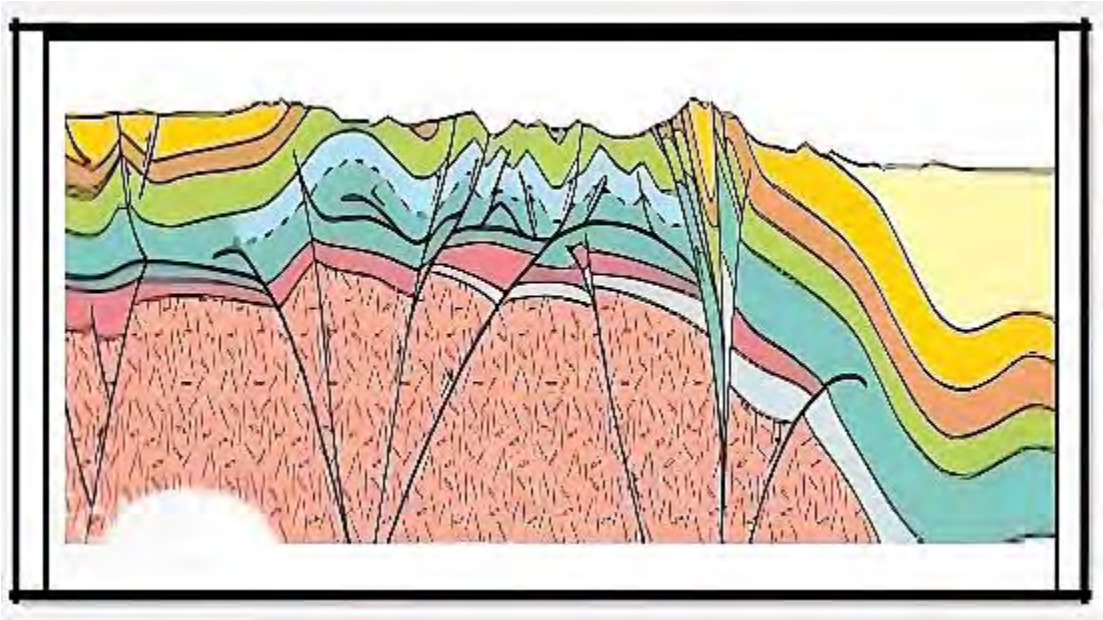

Figure 2.3:Shows Structural pattern of Zamzama Block. (Abbasi et al, 2016).

2.5. Geological Setting

Hydrocarbons, migration, and entrapment are all controlled by the geological environment of a sedimentary basin. According to Kazmi and Jan, Pakistan's geology is separated into two domains: Gandwanian and Tethyan. The Indo-Pak crustal plate supports the southern section of this, which is part of the Gandwanian domain.

This area contains rocks from the Triassic to the Recent epochs. The formation is made up of sand masses that have formed in a variety of shallow marine habitats, from the shoreline to the bottom shelf. During the late Cenozoic, the stronger impact of clastic materials from the north drives the sea to retreat to the south. The Indus basin was occupied with sediments by the end of the Paleocene, and it resembled a large flood plain with braided streams, with the folded belts providing the only height. During the Cretaceous, the Indian Plate drifted and rifted, culminating in the formation of the Lower Indus Basin.

Sedimentary sections from the Tertiary to Mesozoic epochs show adequate sources, possible reservoirs, and caprocks.

2.6. Stratigraphy

The Kirthar Fold Belt Basin's stratigraphic succession is predicted to stretch from Permian to Recent, with substantial unconformities at the Permian, Jurassic, and Upper Cretaceous levels. The Cretaceous rocks in the Suleiman and Kirthar provinces of the Lower Indus Basin are largely sedimentary in origin and, with the exception of small disconformities, form a continuous succession from Early to Late Cretaceous. In some portions of this location, the Tertiary layers are transitional, and local disconformities between the Cretaceous and Tertiary have been identified.

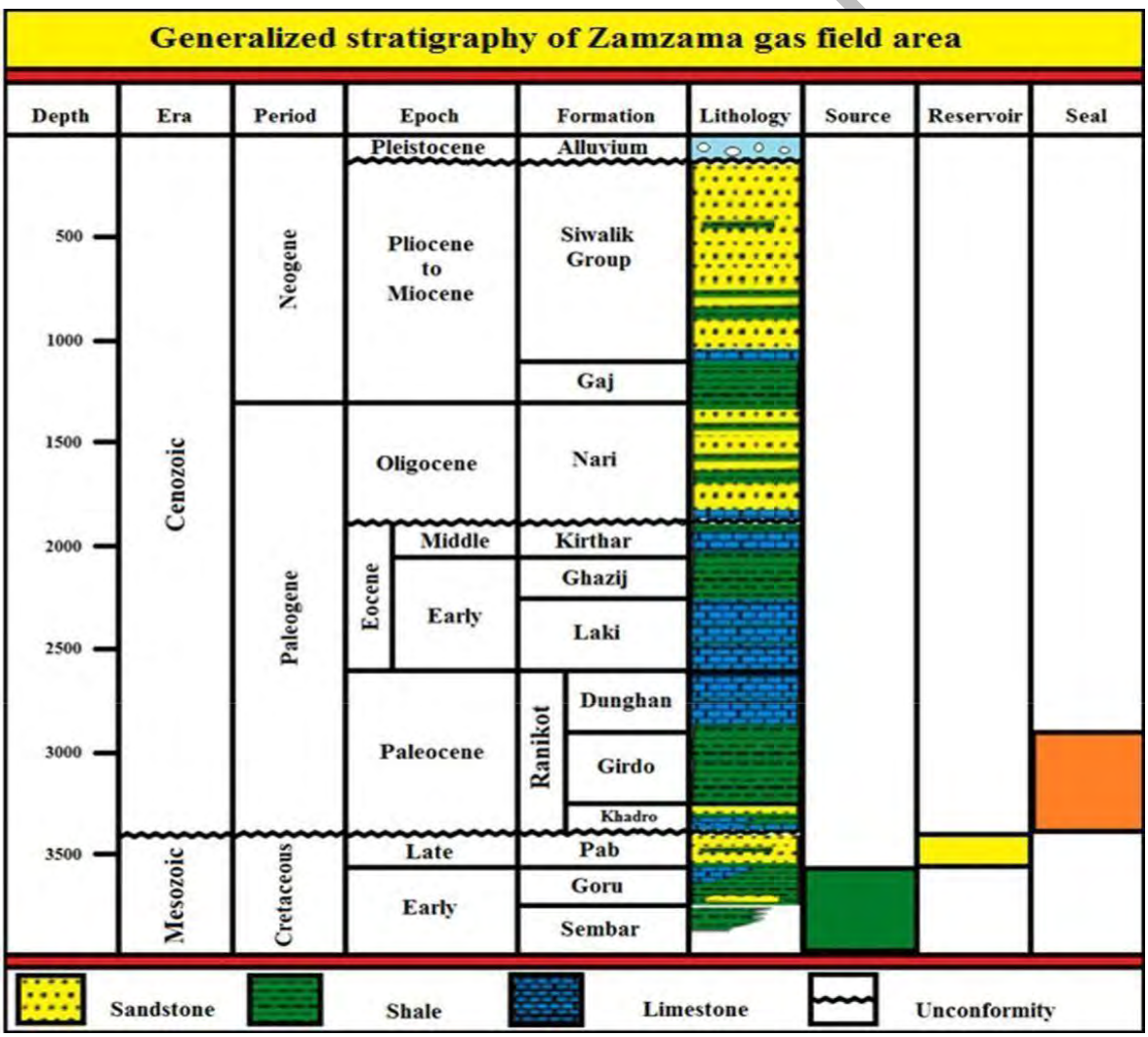

Figure 2.4: General stratigraphy of Lower Indus basin (Abbasi et al., 2016).

The Jurassic sequence is mostly limestone with some shale, whereas the Cretaceous sequence is made up of sandstone, shale, and limestone/marl. Overlain by the Paleocene Khadro, Ranikot, and Dunghan formations, the Cretaceous is unconformable. The Laki, Ghazij, and Kirthar Groups of the Eocene have limestone and shale lithology. Sandstone and shale make up the Oligocene to Pliocene Nari, Gaj, and Siwaliks sequence.

From the well tops, the following Zamzama Block groups and formations can be seen. Figure (2.4) shows a stratigraphic map of the Zamzama block, which is detailed in above figure. Much of the Pab and Mughal Kot Formations, which are widely exposed in western Pakistan, are made up of Late Cretaceous (Companian - Mastrichtian) sandstones. These units, which are dominated by quartos sandstones with subordinate marls and argillites in the southern part of the Kirther Fold Belt, were all deposited on the western continental border of the Indo-Pakistan plate (Khan et al, 2008).

2.7. Petroleum System

With important fields like Zamzama, Bhit, Mazarani, and Sari-Hundi, the Kirthar Fold Belt is a high-volume gas and gas condensate producer, indicate the existence of a dynamic petroleum system in this tectono-stratigraphic province. Except for the Bhit gas discovery, where gas is found in Cretaceous layers, gas discoveries in the Southern Indus Basin are largely from Paleocene deposits (Zaigham and Mallick 2000).

A mature source rock, a conduit to migrate hydrocarbons, reservoir rock, and optimum time for the creation of these elements and the migration processes are all geological components and processes required to create and accumulate hydrocarbons.

2.7.1. Source Rock

The Zamzama Field's source formations are the shales of Cretaceous Sembar and Goru Formations. Goru Formation was deposited in a pelagic environment, whereas the Sembar Formation was deposited on the shelf edge. The majority of the Sembar deposits come from a marine environment. Sembar's TOC ranges from 0.5 to 3.5 percent, with an average of 1.4 percent. The Type-III Kerogen within the Sembar Formation ranges from immature to adult.

2.7.2. Reservoir Rock

Reservoirs Rocks are porous and permeable rocks that have commercial hydrocarbon reserves. The most essential physical features of reservoir rocks for hydrocarbon accumulation are porosity and permeability. The reservoirs in Kirthar Fold Belt are Jurassic to Eocene in age. The fold belt's principal objectives are Middle Jurassic carbonates, Lower and Upper Cretaceous sandstone, Paleocene sandstone and carbonates,

and Eocene carbonates. The principal reservoir for the Zamzama field is the Cretaceous Pab Sandstone. It is found in a tidal and shallow marine environment. The Pab Sandstone is a braid delta/coastal plain deposited formation with a lot of sand.

Limestone from the Kirthar Formation's Habib Rahi and Pirkoh Members could be potential reservoirs in the Eocene. The Pab Sandstone, as well as the sand strata within the Mughal Kot Formation, is the research area's most promising reservoir. Throughout the Sulaiman and Kirthar Ranges, the Pab Sandstone has shown to be a reliable reservoir. Potential reservoirs can be up to 400 meters thick. Sandstone porosities can reach 30 percent, although they're more typical in the 12 to 16 percent range, while limestone porosities range from 9 to 16 percent. These reservoirs have permeabilities ranging from 1 to > 2,000 milidarcies (md).

2.7.3. Cap Rocks

The Paleocene Khadro and Ranikot shale strata operate as a top seal for the underlying Pab Sandstone (Ahmad et al., 2017). These shales have proven to be reliable in bhit, Zamzama, and Mehar fields, among other places. Khadro is sandy in some circumstances and does not operate as an affective seal, whereas Gidro Formation does (Ahmad et al., 2017).

2.7.4. Trapping Mechanism

In the research area, a large N-S trending thrusted anticline acts as a trap (Jackson et al., 2007). On both sides of the fracture, gas was extracted. There is no vertical leakage, however there is cross-wall leakage (Ahmad et al., 2017). In the Zamzama location, the bounding fault does not reach the surface and acts as a seal component (Jackson et al., 2007).

CHAPTER 03

SEISMIC DATA INTERPRETATION

3.1. INTRODUCTION:

The fundamental goal of seismic data interpretation is to estimate hydrocarbon potentials in subsurface sedimentary rock. Searching for hydrocarbons is a risky task. This is the situation since there are no direct ways for discovering hydrocarbons. Because of its high resolution, the seismic reflection method is the essential geophysical approach for exploration. Other methods for prospecting petroleum, such as gravity and magnetic, can also be used. All of these procedures are based on physical principles and qualities that are measured on or below the surface, then interpreted based on what appears below, and geology is inferred through indirect observations. The interpretation is not unique due to the indirect relationship between the surface and depth observations. The analysis of 3D seismic data entails several processes. Different processes were followed to interpret the seismic segment, which included all forms of interpretation. In the oil and gas sector, the fundamental purpose of seismic interpretation is to find and discover the best location for trapped hydrocarbons in a given structure.

3.2. Seismic Data Interpretation:

Seismic data is interpreted by using given approach.

- Structural approach

3.2.1. Structural Interpretation:

The seismic section has a series of reflections that would be examined structurally. Seismic sections are interpreted using the seismic expression of closely adjacent geological sequences. The main aim of seismic interpretation is to mark the structures with in the subsurface using seismic data.

3.3. Workflow Of Seismic Interpretation:

The basic interpretation steps used to interpret the 3D seismic data are as follows.

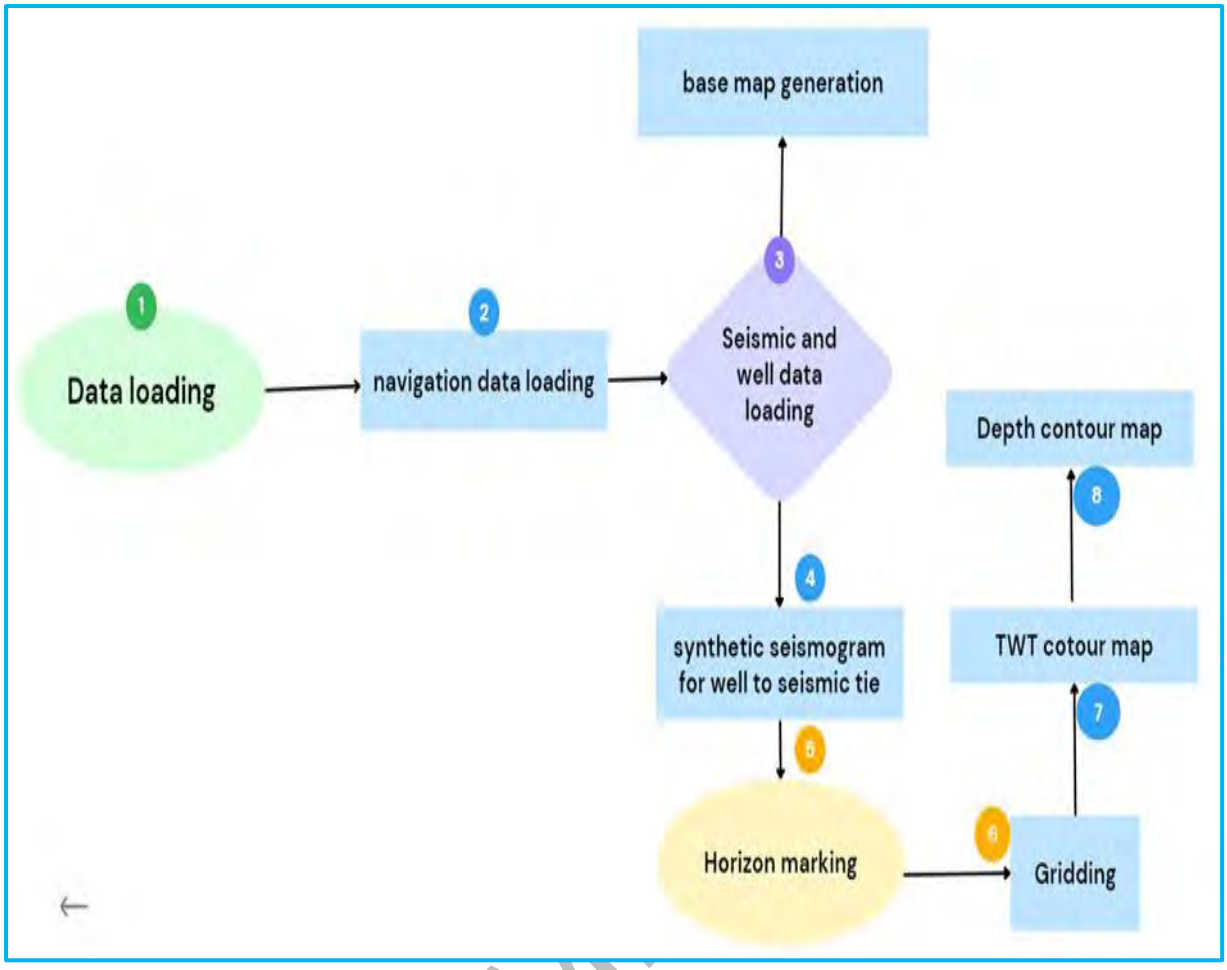

Figure 3.1: workflow of seismic interpretation for Zamzama Gas Field.

3.3.1 Synthetic Seismogram and seismic to well tie:

Based on the well logs (sonic and density) from well Zamzama–03, a Synthetic Seismogram is generated. The horizon is confirmed using the generated seismogram. The following horizons have been chosen:

- Pab Sandstone (Sandstone, Late Cretaceous)
- Fortmunro

Because in-lines lie on the dip of a structure, they are chosen for interpretation. Three-dimensional data has two main faults in our case. Only two reverse faults are linked with the hinge zone of the fold in the Zamzama gas field. Figure 3.2 depicts a Synthetic Seismogram.

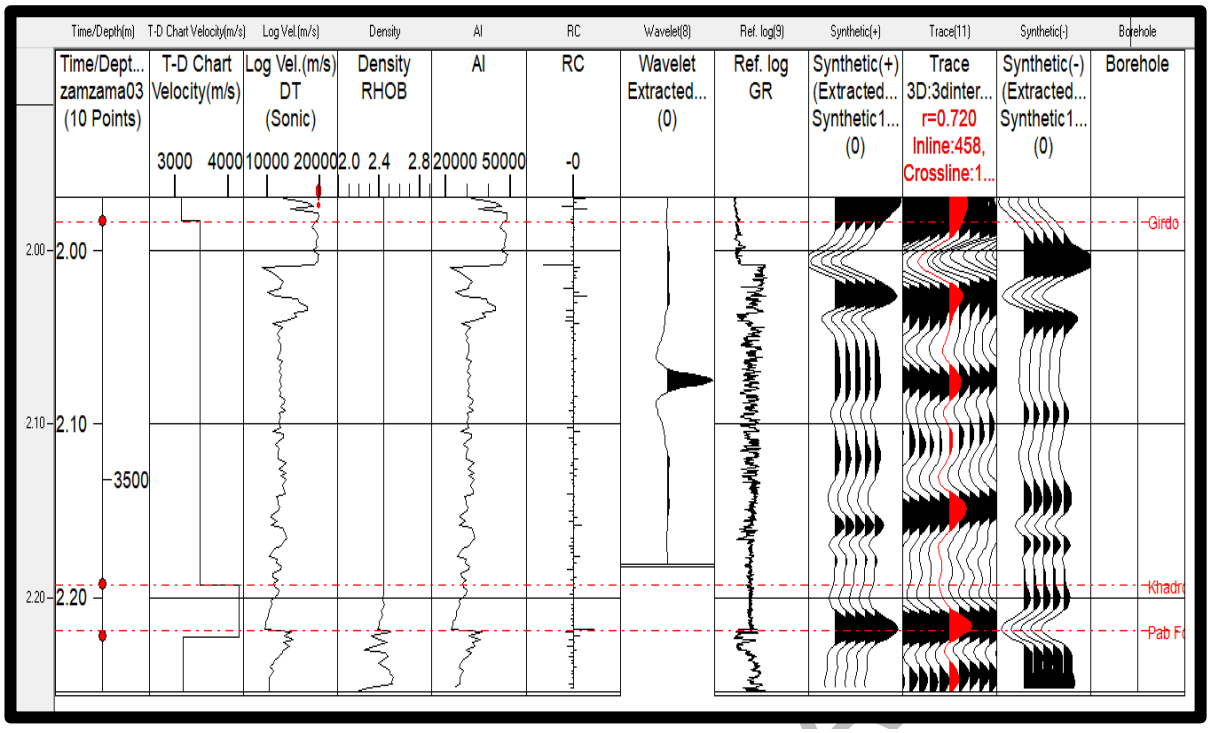

Figure 3.2: Synthetic Seismogram for picking horizons on Zamzama-03 well.

3.3.2 Interpretation Of Horizons And Fault

The horizons were interpreted using the Kingdome IHS programme. The fundamental task of a seismic data interpreter is to interpret horizons on seismic sections. The interpreter is well-versed in the area's structures as well as the geology of the research area. The well tops are correlated with the seismic section to determine the exact location of the horizons on the seismic section. On the basis of the well top of Zamzama-03, two horizons were interpreted on the seismic section. Two Horizons were discovered by combining these Synthetic Seismograms with seismic data in the time domain.

• Pab Sandstone (Sandstone, Late Cretaceous) at 2.2 second .

• Fort Munro (Limestone, Shale, Cretaceous) at 2.36 seconds.

Faults are identified by amplitude decay, reflector discontinuity, distortion, or absence of the reflection. Only two faults, F1 and F2, are marked here, both of which are thrust faults. The marking horizons and faults are shown in the fig 3.3.

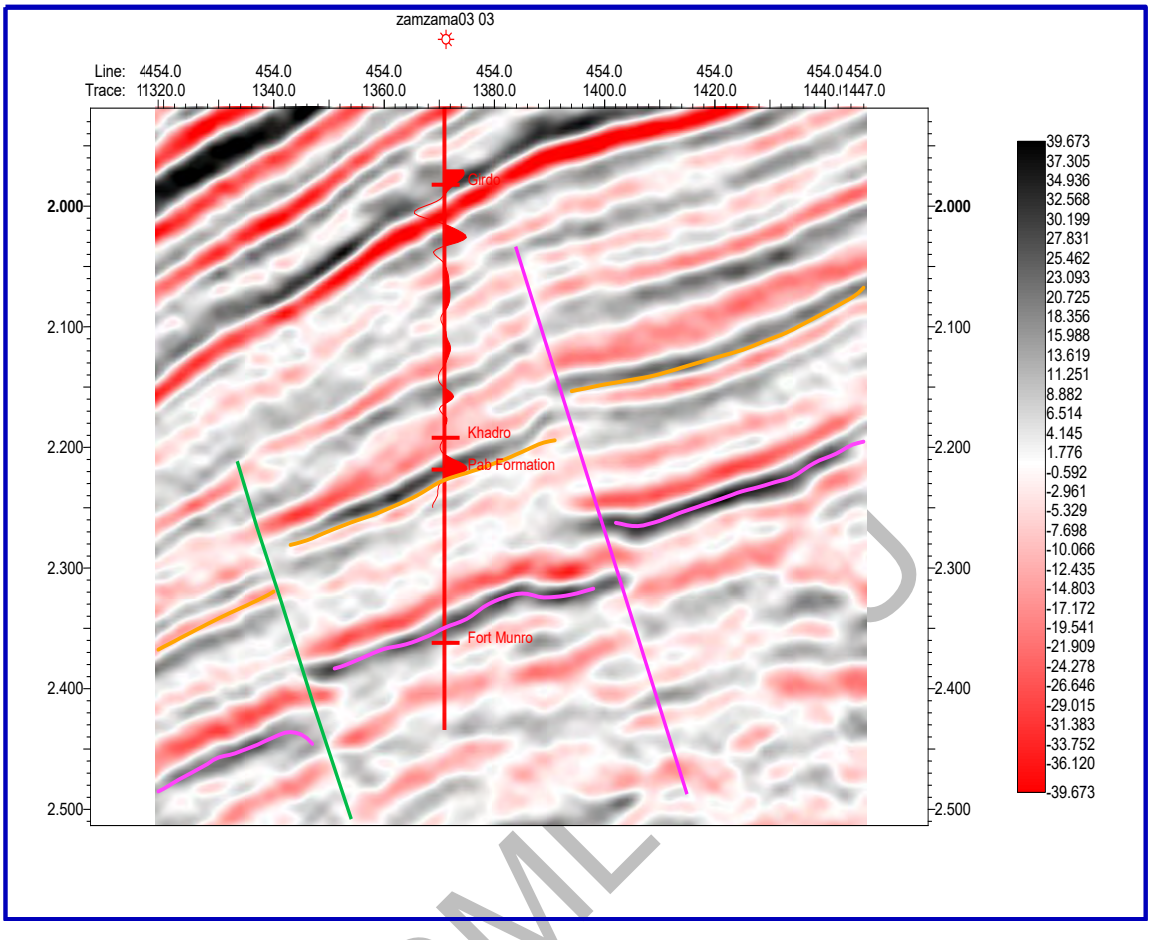

Figure 3.3 : Interpreted seismic inline 451 having faults F1 and F2 and two horizons Pab and Fort Munro.

3.3.2 Construction Of Fault Polygon

To create the fault polygon shown in above Figure 3.3, we must select faults on seismic sections at appropriate intervals, connect them, and cover the space in between for the grids to consider it a faulted area. If we don't transform them into fault polygons, the software won't recognise them as a discontinuity, giving us an inaccurate representation of the area. Figure 3.4 shows fault polygon of Pab Sandstone.

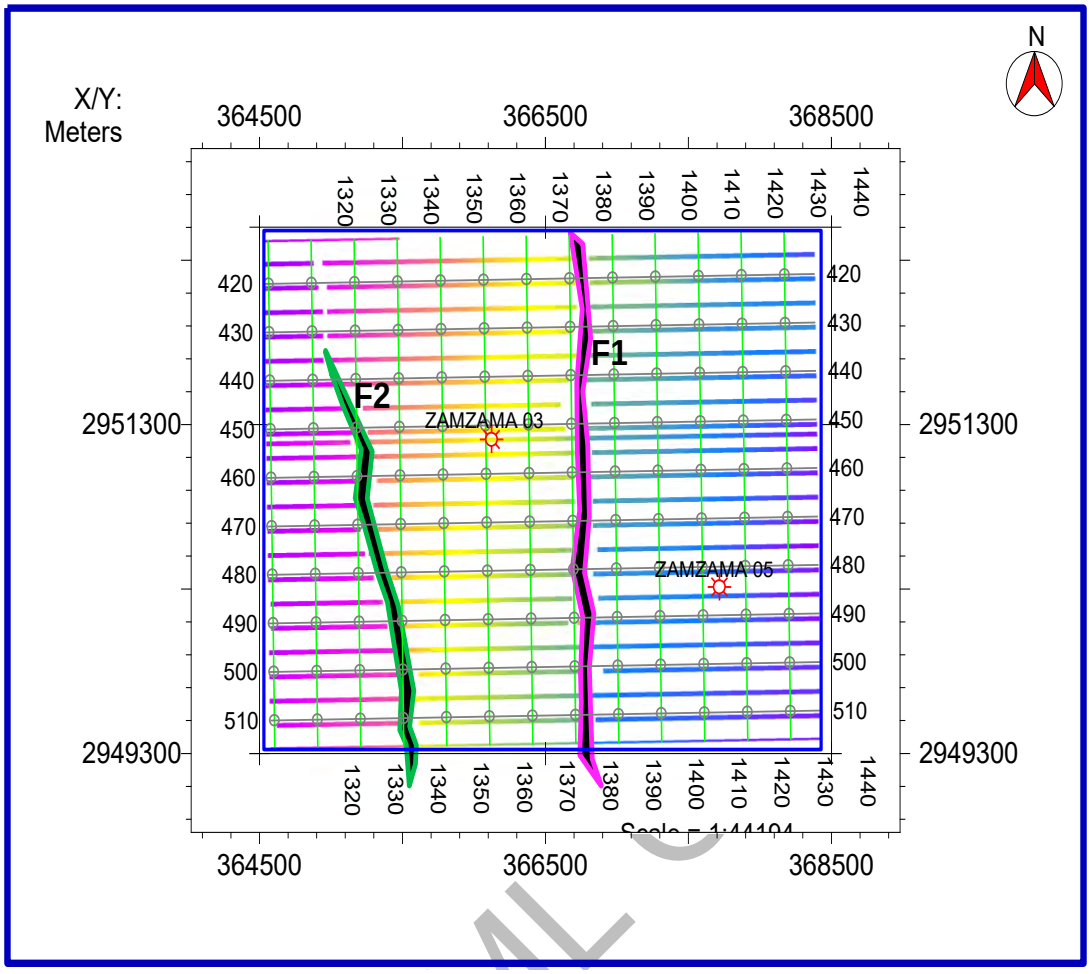

Figure 3.4: Fault Polygon of Faults F1 and F2 along Pab Formation.

3.4 Contour Maps

Contour maps, either in time or depth, are the end results of all seismic exploration. Data mapping is one of the most significant aspects of data interpretation, and it is dependent on the entire operation. Contours are lines that connect points that have similar values (Coffeen, 1986). Contours represent the transformation of a three-dimensional earth surface into a two-dimensional surface. The structural relief of the formation, as well as any faulting and folding, as well as stratigraphic dip, are depicted in these contour maps.

3.4.1 Generation Of Time and Depth Contour maps

The generation of depth and time contour maps is the next step in seismic interpretation. First, time contour maps were created because seismic data is in the time domain, and then depth contour maps were created by transforming seismic data from the time domain to the depth domain using velocity models. Contour lines are data-driven lines of equal depth or duration moving over a map (Coffeen, 1986). The weighted average approach is used to create

the temporal contour maps. This is the best algorithm for places with a lot of complexity, such as Zamzama. The time model's contour interval is 0.008 seconds.

Using the true velocity from wells in the research area, both time contours were translated into depth contour maps by using equation 3.1:

$$s = v * t/2 \quad \text{.....(3.1).}$$

Using KB as a reference data point, depth contour maps were created, and time contour maps were created using the weighted average algorithm. The depth model contour interval is 12.5 meters. The structural relief, formation slope, dip, and any folding and faulting are all visible on these contour maps. These time and depth contour maps were created using Seismic Micro Technology HIS (Kingdom 2017).

The time contour maps of the Fort Munro Formation and the Pab Sandstone were created by marking the two-way time of both formations on seismic sections and contouring them. A flank or limb of an anticline structure is found in the Zamzama area, as shown by the two-way time contour and their trend on the seismic section.

3.4.2 Pab Sandstone

The below shown Figures 3.5 and 3.6 shows the time and depth contour maps of Pab Sandstone. The blue colour in time contour map indicate the lowest time and the pink color show highest time which shows the deepest part indicating the flank or limb of an anticlinal structure.The blue colour in depth contour map shows lowest depth and the pink color indicates highest depth. The sinking limb of an anticline running from north to west is seen on the time and depth contour maps. It is depicted that the Pab Sandstone is a flank or limb of an anticline-like structure by employing colour contrast and contour trends.

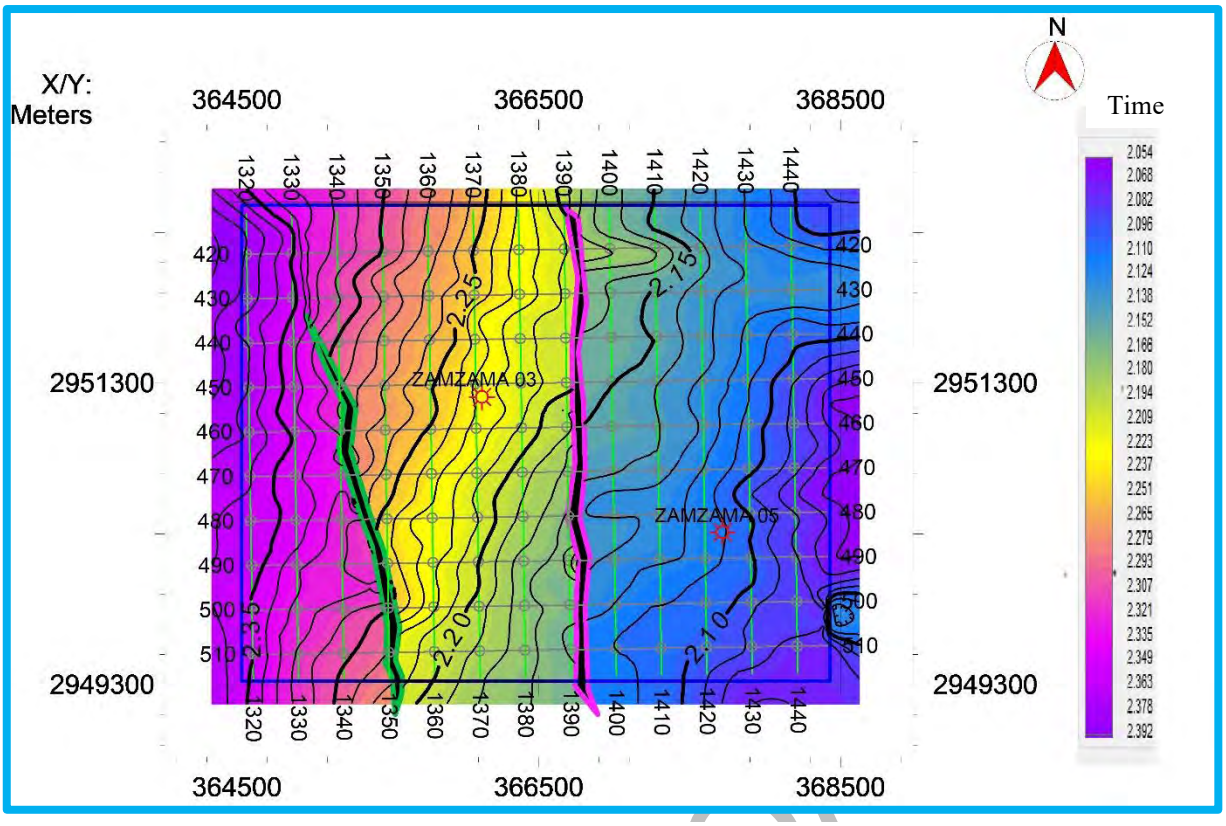

Figure 3.5: Time contour map of Pab Sandstone.

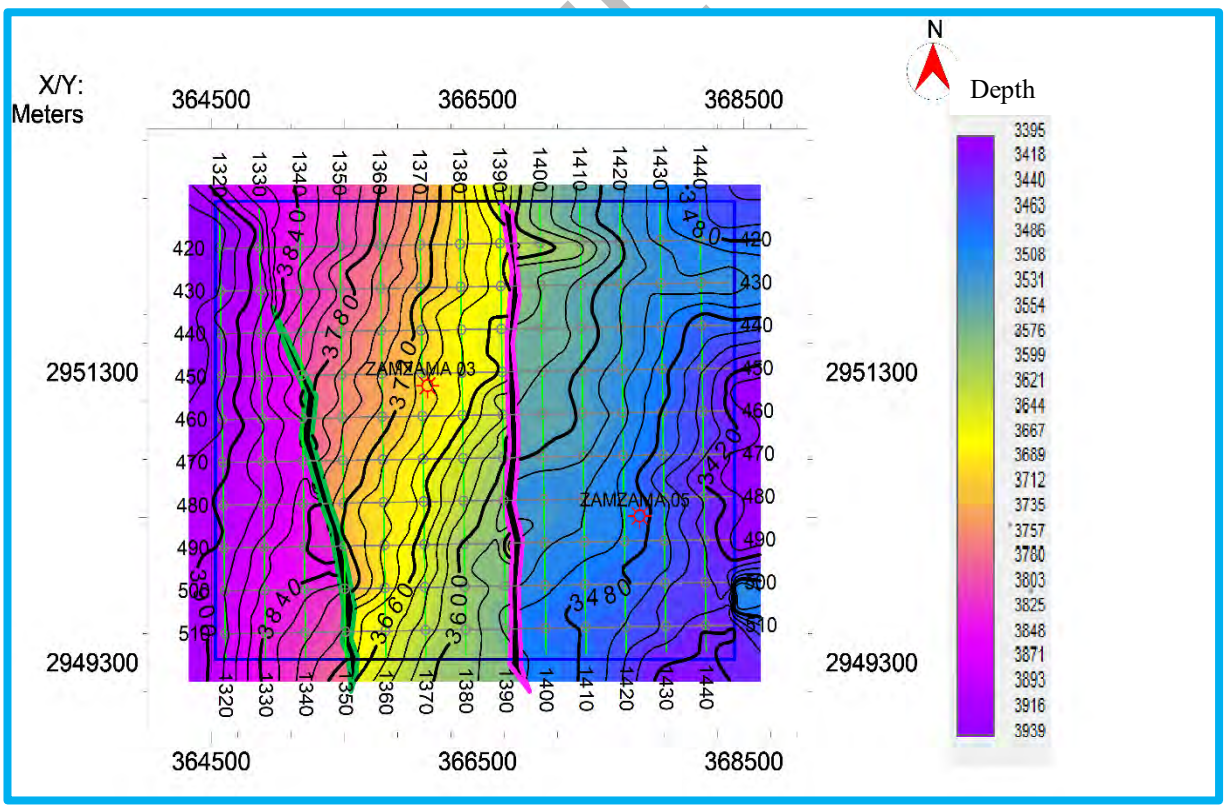

Figure 3.6: Depth contour map of Pab Sandstone.

CHAPTER 04

PETROPHYSICAL ANALYSIS

4.1 Introduction To Petrophysical Analysis

For petroleum geoscientists, petrophysics is a crucial technique. It is used to correlate wire-log data, create structure maps and isopach maps, calculate the porosity and permeability of rock formations, pinpoint the locations of hydrocarbon-bearing zones, and analyse the lithology and pore geometry of the rocks.

Geophysicists study the physical characteristics of the reservoir, such as fluids in the rock body, in petrophysics. A geophysicist may then depict the reservoir, which is the crucial phase in the oil and gas sector. It assists in identifying well-potential and hydrocarbon-bearing zones, which aids in determining the wells' economic value.

Petrophysics is an analysis done on data from well logs. Well logs are analysed in petrophysics. Well logs are measurements of the physical and chemical characteristics of the rock taken along the depth of the well. "Sonde" equipment, which monitors the physical and chemical characteristics of the rock and how they interact with fluids, is used for well logging (Rider, 1986).

The importance of petrophysical analysis has increased as a result of recent developments in logging tools that have improved the quality of well log data. In the petroleum business today, productive zones, reservoir oil and gas levels, and the presence of economically viable hydrocarbon reserves can all be predicted using wire-log analysis.

Petrophysical analysis has made new methods for predicting the pore pressure of underground rock possible. These methods aid in reservoir maintenance and the avertance of well blowouts. Calculations should be made with accuracy for the reservoir's physical characteristics like shale volume and fluid saturation. In order to get the best return on our investment and meet safety standards, one can monitor, stimulate, and boost reservoir production with the use of petrophysics.

4.2 Petrophysical Analysis WorkFlow

Petrophysical analysis is used to examine the reservoir of well Zamzama-03 in the Dadu area of the Lower Indus Basin. The petrophysical analysis workflow chart is illustrated in Figure 4.1.

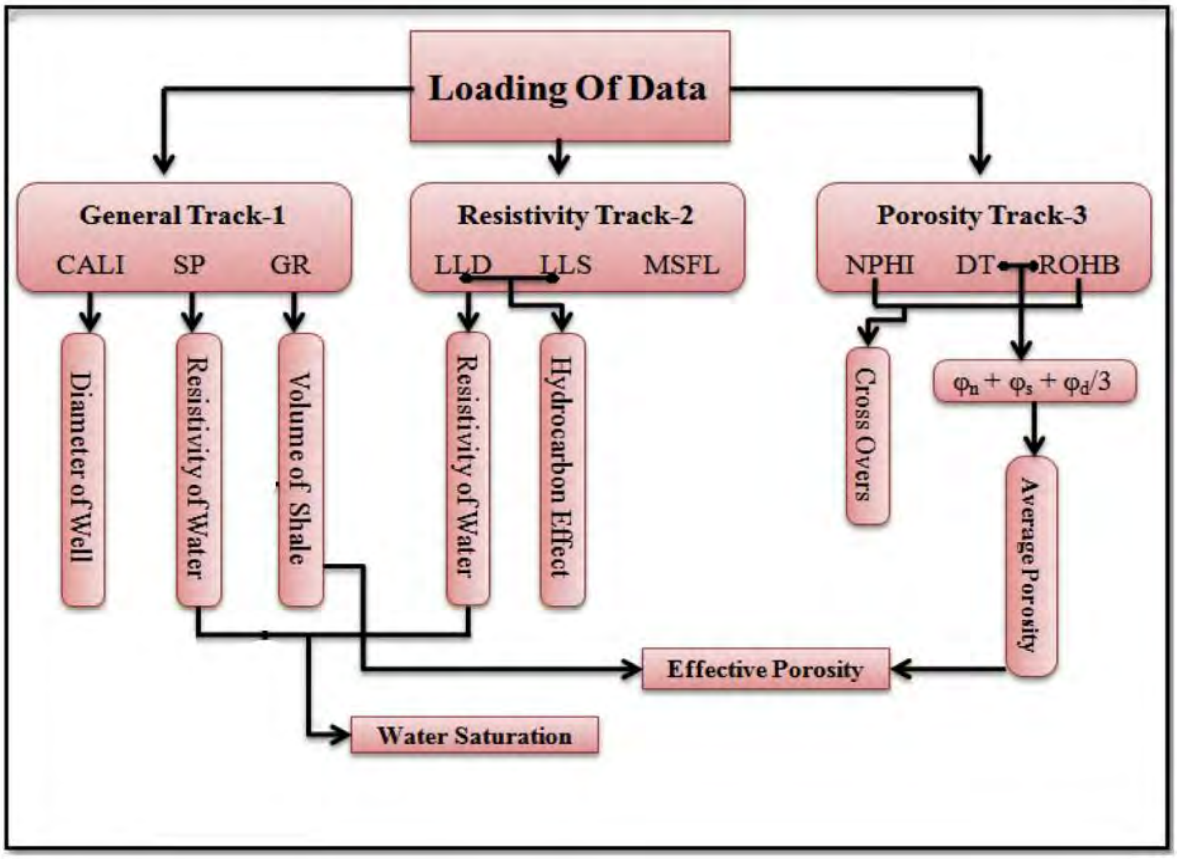

Figure 4.1:Depicts the petrophysical interpretation workflow.

4.2 Logs used in petrophysical analysis

Spontaneous Potential (SP) log, Caliper log, Sonic log, Gamma Ray (GR), Density, Resistivity, Neutron, Latero shallow (LLS), and Latero deep logs log (LLD) are used for petrophysical analysis. Three tracks, the lithology, porosity, and resistivity tracks are used to present these logs. Gamma ray, Caliper, and SP logs are all included in the lithology track. LLD and LLS are used in resistivity track. Density, Sonic and Neutron logs are used in porosity track.

4.3 Calculated Parameters

Following parameters are calculate for petrophysical analysis:

- Volume of shale.
- Density porosity.
- Effective porosity.
- Water saturation.
- Hydrocarbon saturation.

4.3.1 Volume of Shale

Shale volume is primarily determined using the GR log. The radioactive elements were exclusively present in shale and absent from sand, which is referred to as clean sand is used for the quantitative calculation of shale volume.

The electromagnetic particles that are expelled from the formation are measured by the GR log. They are referred to as photons. The GR log, also known as the particle count and display, shows these particles every second. Sand and shale are often separated using the GR log (Fischetti, 2002).

The formula below can be used to calculate the amount of shale in the formation (Asquith and Gibson, 2004). Equation 4.1 and 4.2 gives the volume of shale equation.

$$V_{sh} = \frac{GR\ log - GRmin}{GR\ max - GRm_in} \quad \text{.....4.1}$$

$$V_{sh\_Stieber} = \frac{IGR}{3-2*IGR} \quad \text{.....4.2}$$

Where

Vsh = Volume of shale

$GRlog$ = Reading of GR log at that point

$GRmin$ = Minimum value of GR log

$GRmax$ = Maximum value of GR log

4.3.2 Porosity calculation

By dividing the volume of the pores by the entire volume of the formation, porosity will be calculated. The porosity of rock formation is determined using neutron, density, and sonic logs.

Sonic porosity

A transmitter and receiver comprise the instrument used to read sonic logs. The sound waves are transmitted along a rock formation in a well, and the receiver detects them as they return after reflection. This tool measures the transitory time by timing how long it takes for waves to cross a formation one foot at a time. The transient time interval is influenced by the lithology and porosity of the underlying rock (Fischetti, 2002).

Sonic porosity is calculated by:

$$\Phi s = \frac{\text{DTlog} - \text{DTmatrix}}{\text{DTfluid} - \text{DTmatrix}} \quad \text{.....4.3}$$

where,

Φs = sonic porosity

DTlog = Transient time of rock formation

DTmatrix = Transient time of matrix only

DTfluid = Transient time of fluid only

Neutron porosity

The concentration of hydrogen ions in the rock formation is determined by the neutron log. In this record, neutrons are released by the sonde as it lowers into the borehole; following their release, these neutrons contact hydrogen atom nuclei that are stored in the fluids within the pores of the formation, causing some of their energy to be lost. Formation porosity is related to this energy loss (Asquith and Gibson, 2004). When clean sand is filled with water or another liquid, the neutron log measures the porosity that is filled with the liquid. Gas molecules contain less hydrogen than oil molecules, which results in relatively low porosity values. Low neutron porosity values are caused by the presence of gas in the formation and are referred to as the gas effect (Asquith and Gibson, 2004).

Density porosity

Knowing the type of rock allows for the calculation of the porosity, which in turn depends on the density of the rock (Asquith and Gibson, 2004). The bulk density, fluid in formation density, and the combined density of the grain are all recorded in the density logs. The equation represents the density porosity of the formation as calculated using the formula below (Asquith and Gibson, 2004).

$$\Phi d = \frac{\rho_{mat} - \rho_b}{\rho_{mat} - \rho_{fl}} \quad \text{.....4.4}$$

where,

Φd = Density porosity

ρ_{mat} = Density of rock matrix

ρ_b = Bulk density

ρ_{fl} = Density of fluid in rock pores

4.3.3 Average Porosity

The average total porosity is computed by dividing all porosities by the total number of logs because different logs are used to compute the porosities of different logs. The relationship depicted in the equation is used to calculate the Pab Sandstone's overall average porosity.

$$\Phi_{avg} = \frac{\phi_n + \phi_d + \phi_S}{3} \quad \text{.....4.5}$$

where,

Φ_{avg} = Average porosity

ϕ_n = Neutron porosity

ϕ_d= Density porosity

ϕ_S = Sonic porosity

4.3.4 Effective porosity

Effective porosity gives the porosity of voids which are interconnected. Effective porosity is used to estimate hydrocarbon and water saturation. Effective porosity can be calculated by following equation (Aquith and Gibson, 2004).

$$\phi_e = \phi_t * (1 - VSH) \quad \text{.....4.6}$$

where,

ϕ_e = Effective porosity

ϕ_t = Total porosity

VSH = Volume of shale

4.3.5 Resistivity of Water

Applying several techniques, the water resistivity can be estimated. The resistivity of fluids and the resistivity of formation can both be calculated using two experiments. The first test is a direct measurement; during this test, an electric current is passed between two electrodes on logging equipment, and the potential drop between them gives us the resistivity. In the second test, which is an indirect measurement, the conductivity is measured by inducing a current in the borehole's formation and detecting how well it can carry the current. After that, the resistivity can be computed by taking its inverse (Krygowski, 2003).

The following Figure 4.2 is used to calculate the Rmeq, while the Figure 4.3 is used to calculate the resistivity of water.

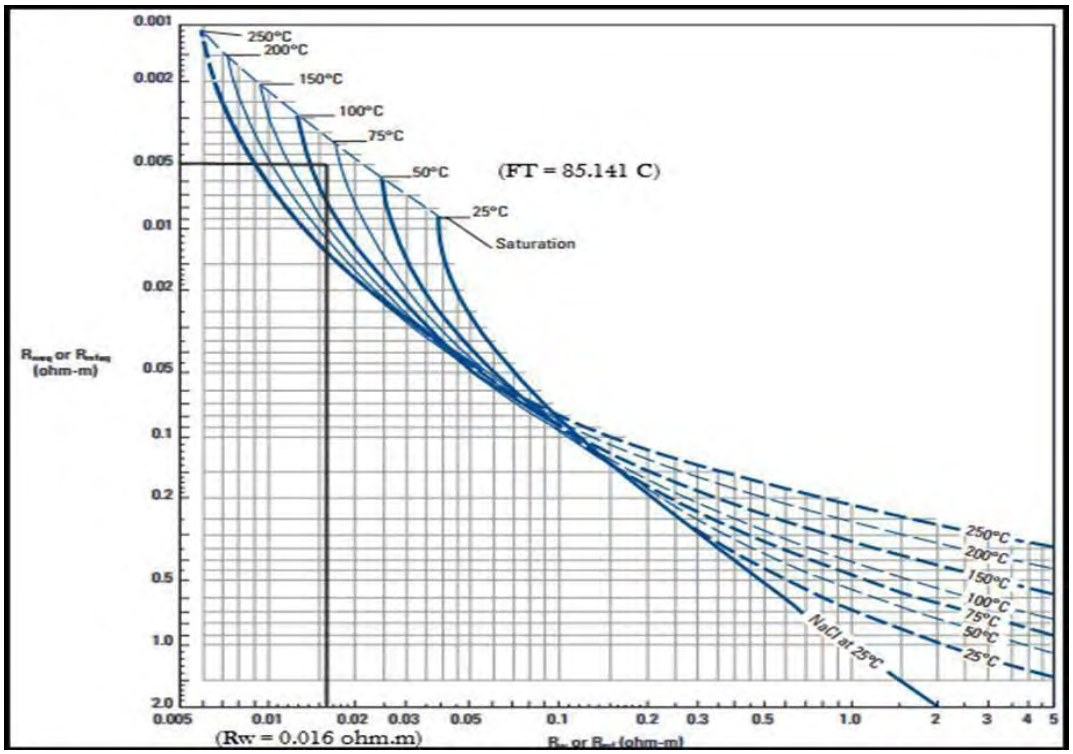

Figure 4.2: Determination of Rmeq from SP chart (Schlumberger, 1989).

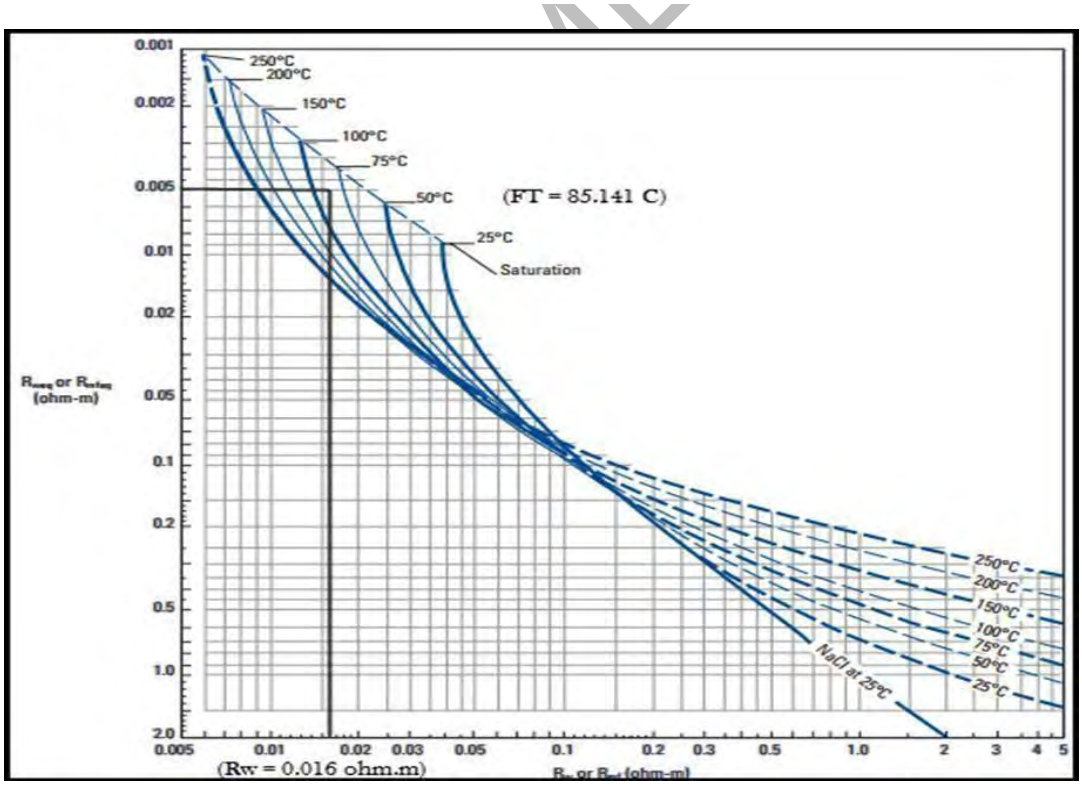

Figure 4.3:Determination of Rw from SP chart (Schlumberger, 1989).

4.3.6 Water Saturation

The percentage of voids in a rock's formation that are filled with water is called water saturation. Water saturation is computed by using the Archie equation.

$$S_w = \sqrt{\frac{a*R_w}{\emptyset^m*R_t}} \quad \text{.....4.7}$$

where,

"a" = Tortuosity factor

Sw = Water saturation

Φ = porosity

Rt = Resistivity of formation

Rw = Resistivity of formation water

m = Cementation factor

n = Saturation exponent

4.3.7 Hydrocarbon Saturation

Hydrocarbon saturation represents the presence of hydrocarbons in the pore spaces of rock formations. "Sh" stands for the saturation of hydrocarbons (Kamel and Mabrouk, 2002). A given equation is used to determine the amount of hydrocarbon present in the void spaces.

$$S_h = 1 - S_w \quad \text{.....4.8}$$

where,

S_h = hydrocarbon saturation

S_w = water saturation

This technique, which is indirect, reveals the remaining hydrocarbon content in the voids.

4.4 Well Log Interpretation of Zamzama –03

The Kingdom Software is used for petrophysical interpretation of well Zamzama - 03 to determine the hydrocarbon zones. Figure 4.4 displays every log. The zone 1 marked as a zone of interest, as seen in figure 4.4. This zone is 20 metres thick, with a depth between 3700 and 3720 metres. Due to the minimal radioactive material and low shale volume in a suitable reservoir, this zone exhibits low GR log and shale volume values, revealing clean sand. Because LLD has higher values in the reservoir than LLS log, there is a distinct separation between LLD and LLS, indicating that the zone of interest may be a reservoir that contains hydrocarbons.

Additionally, there is overlap between NPHI and PHID. Since hydrogen ion concentration in the formation is used to measure neutron porosity and hydrocarbons contain

fewer hydrogen ions than water, the presence of hydrocarbons may be indicated by this. The zone of interest has a high effective porosity. The zone of interest also exhibits significant hydrocarbon saturation and low water saturation. Based on all of these findings, the zone indicated is most likely a hydrocarbon saturation zone. Calculated values of Pab Formation at reservoir zone of Zamzama 03 well is shown in table 4.1.

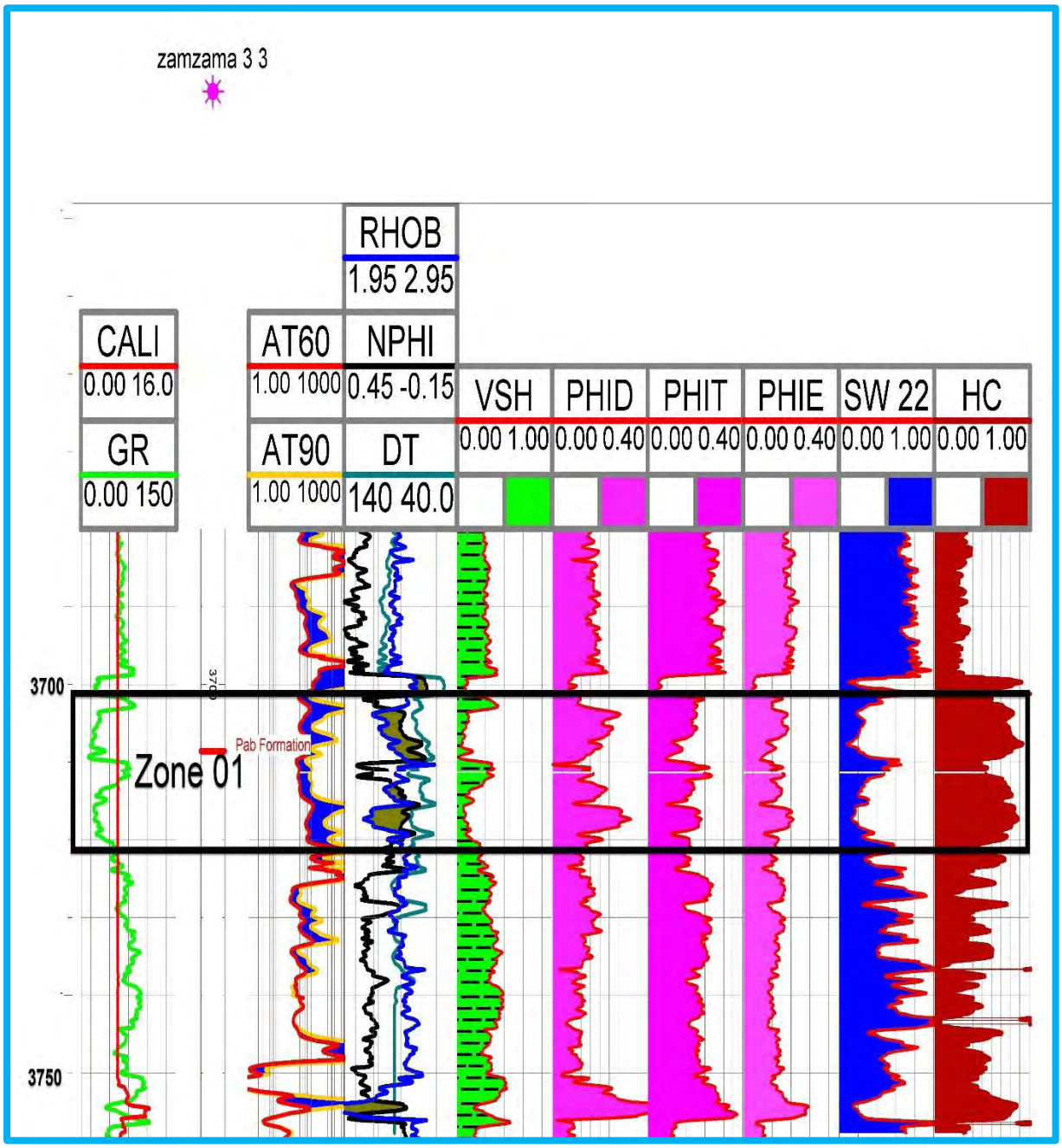

Figure 4.4:Well log interpretation of well zamzama 03.

Table 4.1:Calculated values of Pab Formation at Zamama 03 well.

	Zone 1
Gross Thickness	3700-3720 (20m)
Volume Of Shale	21%
Effective Porosity	10%
Water Saturation	24%
Hydrocarbon Saturation	76%

CHAPTER#05

ROCK PHYSICS MODELLING

Essentially, rock physics modelling gives the link between seismic and rock features. Seismic waves can travel to considerable depths within the ground because they have a low frequency and a high amplitude. We employ rock physics modelling to link seismic to rock properties and quantitatively interpret the rock because seismic cannot resolve the underlying properties of rock and even thin beds are not identified by seismic.

5.1 Bulk density and compressional and shear wave velocities

Velocities and densities used in seismic models for exploration are typically derived mostly from wireline log data. Particle motion inside the P-wave-driven wave transmission trend. The S-wave travels down the same path as the P-wave (but at half the speed of the compressional wave), but the motion of the particles is at an angle to the direction of wave propagation. Bulk Density is a fairly straight forward variable that is calculated as the weighted average of the component densities.

5.2 Calculation of elastic moduli

Understanding the isotropic and elastic context of velocities and density is also necessary in order to comprehend the rock physics tools of seismic methods because we completely concentrated on porosity and density in Petrophysics (Simm et al. 2014).

Numerous elastic parameters can be used to explain the isotropic and elastic behaviour of rocks. Any other elastic parameter can be calculated from any two independent measurements. In this study, compressional and shear wave velocities are used to measure additional elastic moduli. Rocks' responses to different stresses are described by elastic moduli.

Compressional Sonic log from wells Zamazam-03 and Equation 5.1 are used to calculate Vp log, which reveals that sonic is measured in microseconds per foot and Vp is measured in metres per second.

Vp= (10°/3.28 DT)……..5.1

In order to determine the Vs, the well Zamazam-03 provides both shear and compressional logs. By using Vp and Vs log we calculate different moduli which are briefly explained below.

5.2.1 Bulk modulus

It is the ratio of volumetric strain to stress. A substance's bulk modulus evaluates its response to uniform compression and explains how it reacts to uniform pressure. Bulk modulus can be calculated by using equation 5.2.

$$K = \rho(v_p^2 - \frac{4}{3}v_s^2) \quad \text{.....5.2}$$

5.2.2 Young's modulus

The ratio of linear stress to linear strain is known as the Young modulus within the elastic limits where Hook's law is applicable. Young's modulus is a measurement of a material's stiffness that is isotropically elastic. We obtained Young's modulus from the logs of Vp and Vs using the relation shown in equation 5.3.

$$E = \frac{\rho v_s^2(3v_p^2 - 4v_s^2)}{v_p^2 - v_s^2} \quad \text{.....5.3}$$

where,

v_p = p-wave velocity

v_s = s-wave velocity

ρ = Density

5.2.3 Poisson's ratio

The Poisson's ratio is the ratio of transverse strain to longitudinal strain. A material sample expands in one direction and contracts in the other direction, and vice versa. This tendency is measured by the Poisson's ratio. The Poisson ratio controls the relationship between two wave velocities (PR). The elastic moduli formulas were used to determine the Poisson's ratio from the Vp and Vs logs, which has a range of 0 to 0.4. Lambda row and meu row has been further calculated for crossplot analysis.

The impedance is measured in (m/s*g/cc) and the modulus is measured in (MPA) units.

$$Al = Vp * p \quad \text{.....5.4}$$

We used Kingdome Software (IHS) to calculate all the properties using all the elastic moduli, and we then represented the curve using several tracks. The Acoustic Impedance was calculated using the 5.4.

By dividing the compressional wave by the shear wave, the Vp/Vs ratio is determined. Since Vs does not pass through the fluid contents and remains constant, Vp should be reduced for a

high potential gas sand reservoir zone. As a result, the Vp/Vs ratio will be in the range of 1.2 to 1.8, and P- Impedance will be low.

The Zamzma-03 zones of interest are shown in Figure 5.1. Based on moduli and petrophysical characteristics two zones are marked. The high-potential zones are shown in figure 5.1. In the reservoir zone, the Poisson ratio decreases as well as compressional velocity, Vp/Vs Ratio, Acoustic Impedance, bulk, and young modulus all decreases. Also GR value is low which shows volume of shale is quite low. Effective porosity is high in reservoir zone and water saturation depicts low values, indicating that selected zone fulfills all requirements for potential hydrocarbon zone.

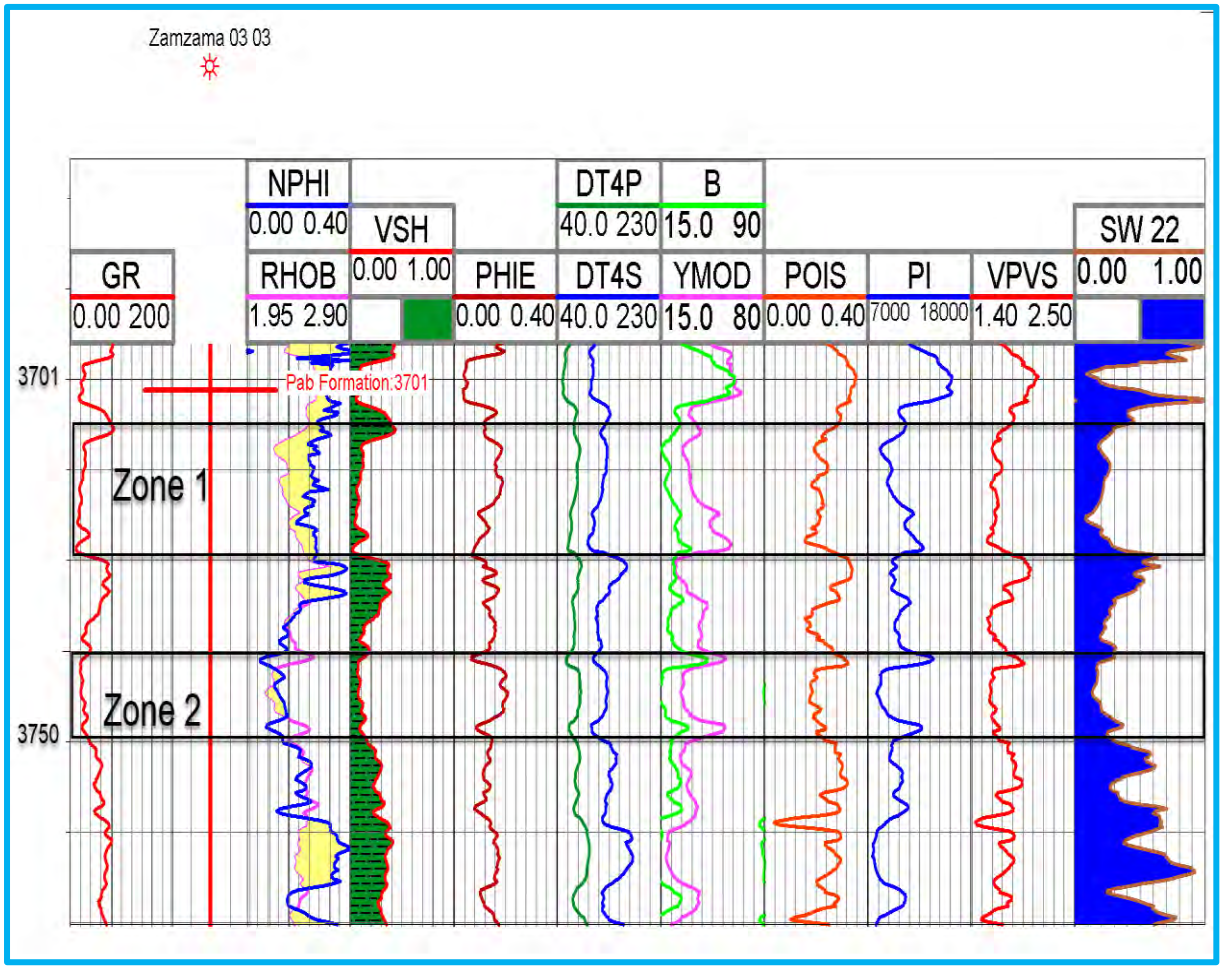

Figure 5.1:Modulli calculation of high potential zones indicating zone of interest.

5.3 Vp/Vs ratio verses Acoustic Impedance cross plots

For lithology determination, sonic time is a porosity tool that is frequently employed. Rock properties can also be ascertained using S-wave time travel. Compressional waves are significantly influenced by the fluid. The compressional and shear ratio, often known as the "Vp/Vs ratio," is a useful characteristic for figuring out the lithology and fluid types.

High hydrocarbon saturation (Sh) causes Vs to increase and Vp to decrease. Compressional wave travel time records can be used to evaluate the porosity and lithology of a rock. S-wave velocity can also be used to recognize rock crystals and calculate porosity. S-wave travel duration is advantageous to fluids. Some data suggests that S-wave travel time may be helpful for fluids. Combining S-wave and P-wave data makes it easier to identify fluid forms, especially in gas reservoirs (Simm et al. 2014).

The final result of modelling is a rock physics template that shows how seismic characteristics, lithology, and saturation relate to one another. The rock physics template is a set of instruments for deciphering well lithology and pore fluid. These templates are frequently interpreted using cross plots of the Acoustic Impedance and the vp/vs ratio. The velocity and porosity trends for the anticipated lithology can be found in the portion of the rock physics template (Avseth and Odegaard, 2004).

The effects of basin constraints on a point in the Rock physics template are as follows:

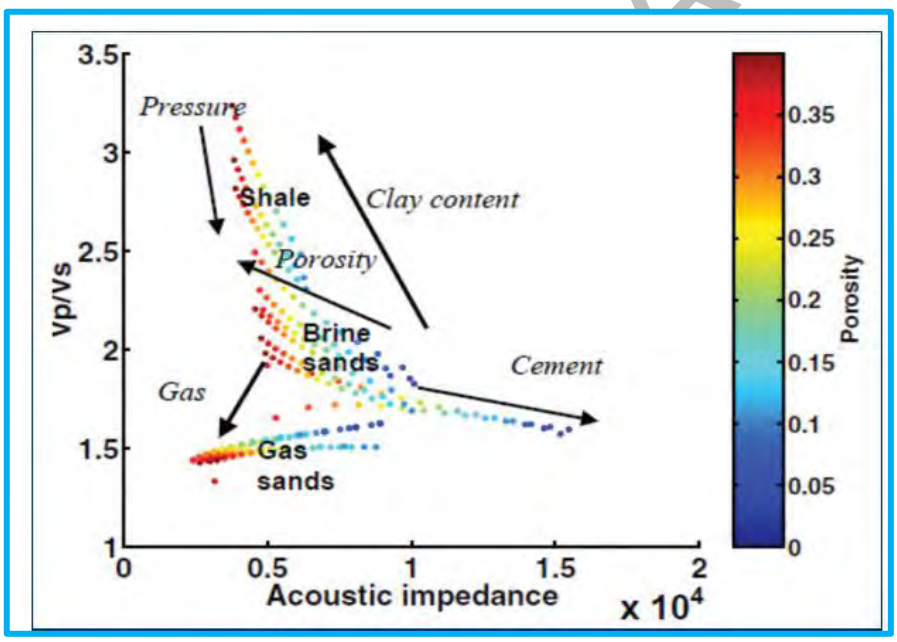

Figure 5.2:Rock physics template (Odegaard and Avseth, 2004).

• As gas saturation rises, the P-Impedance and Vp/Vs ratio will decreases.

• Cement rate increases, Acoustic Impedance increases, and the Vp/Vs ratio decreases.

• As porosity rises, the Vp/Vs ratio rises while the P-Impedance decreases.

• As the amount of shale grows, the Acoustic Impedance will fall as the Vp/Vs ratio rises

5.3.1 Crossplot analysis using PHIE at Z-axis

The relationship between the Crossplot of Vp/Vs verses AImp, shear impedance verses bulk modulus, Vp/Vs ratio verses lambda row and shear impedance verses Aimp is shown in Figure 5.3. In figure 5.3 four figures has been shown. In figure (a) a polygon is marked for the 1.5 to 1.8 range of the Vp/Vs ratio and low values of P-impedance, and PHIE provides colour labelling. A polygon is used to indicate the values where the PHIE gives high values, p-impedance and Vp/Vs ratio all provide low values. PHIE is used for colour coding, as seen in figure (a).

Figure (b) shows crossplot of shear impedance verses bulk modulus. The marked polygon shows that shear-impedance and P-impedance gives low values , PHIE is used for colour coding which predicts that marked zone is gas bearing zone.

Figure (c) depicts the crossplot of Vp/Vs ratio verses lambda row. The potential hydrocarbon zones must gives low values of Vp/Vs ratio and low to moderate value of lamda row a, which is marked by polygon as shown in figure (c).

Figure (d) gives the crossplot of shear impedance verses Aimp. For gas bearing zone shear impedance and p-impedence is always on lower side. The marked polygon in figure (d) completely depicts the gas bearing zone.

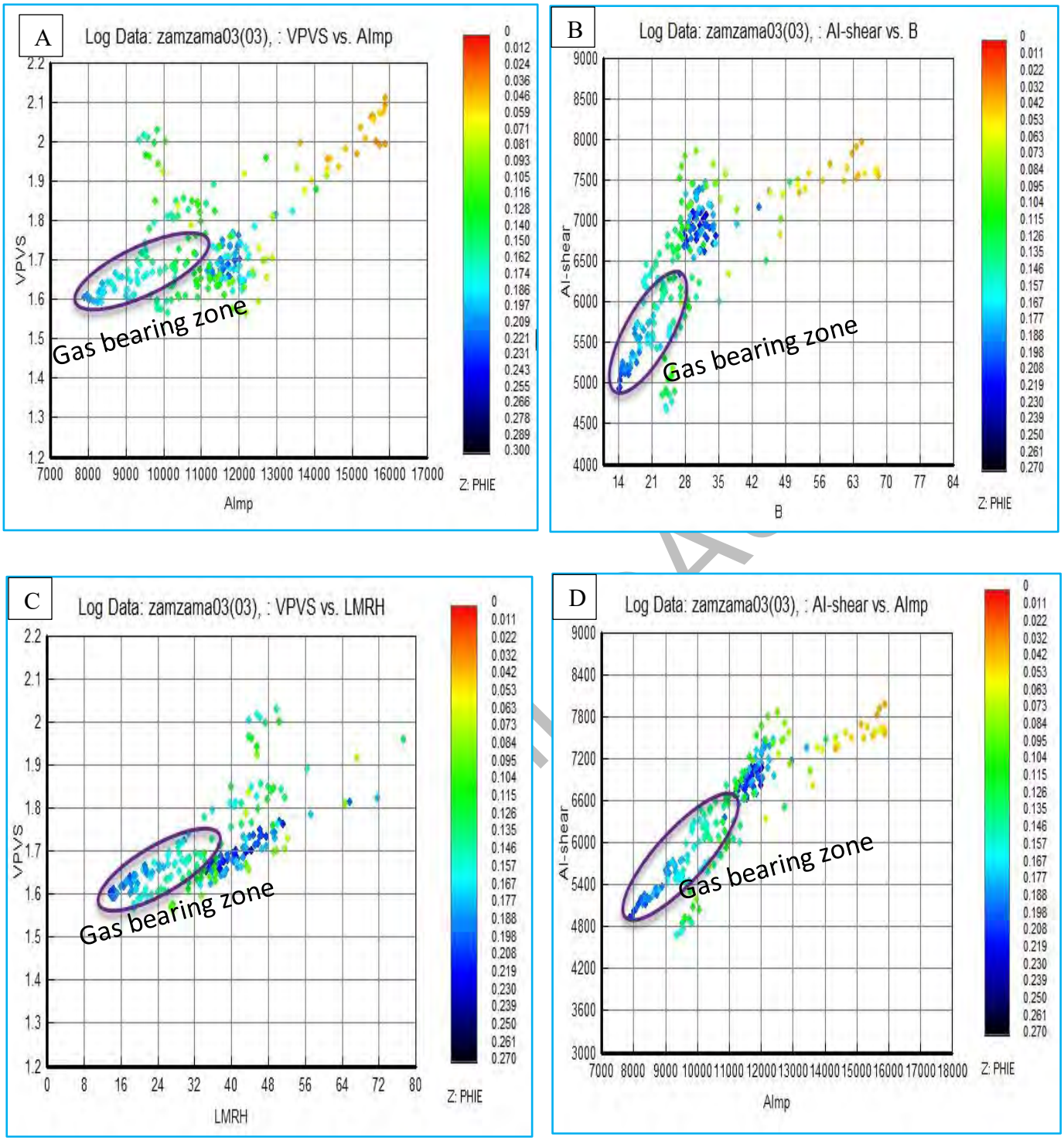

Figure 5.3: The crossplot analysis using PHIE at z – axis with marked gas bearing zone (A) v_p/v_s verses Aimp, (B) AI-shear verses bulk modulus, (C) v_p/v_s verses lamda row, and (D) AI-shear verses Aimp.

5.3.2 Crossplot analysis using Vsh at Z-axis

The VpV's ratio is used as a lithology indication tool in the exploration sector. Geophysicists recommend that the VpV ratio be between 1.6 and 1.7 for sandstone, 1.8 for dolomite, and 1.9 for limestone (Simm 2014).

Figure 5.4 depicts the relationship between Crossplot of Vp/Vs verses AImp, shear impedance verses bulk modulus, Vp/Vs ratio verses lambda row and shear impedance verses Aimp. Four figures are given in figure 6.4. In figure (a), a polygon is designated for the low values of P-impedance and the 1.5 to 1.8 range of the Vp/Vs ratio, and Vsh provides colour labelling. The values where the Vsh, P-impedance, and Vp/Vs ratio all produce low values are marked with a polygon, indicating that marked zone is gas bearing zone. As seen in figure(a), colour coding is done using Vsh.

Figure (b) shows shows crossplot of shear impedance verses bulk modulus. The marked polygon shows that shear-impedence and P-impedance gives low values , Vsh is used for colour coding which predicts that marked zone is gas bearing zone.

Figure (c) depicts the crossplot of Vp/Vs ratio verses lambda row. The potential hydrocarbon zones must gives low values of Vp/Vs ratio and low to moderate value of lamda row which is marked by polygon as shown in figure (c).

Figure (d) gives the crossplot of shear impedance verses Aimp. For gas bearing zone shear impedance and P-impedence is always on lower side. Vsh is used for colour coding. The marked polygon in figure (d) completely depicts the gas bearing zone.

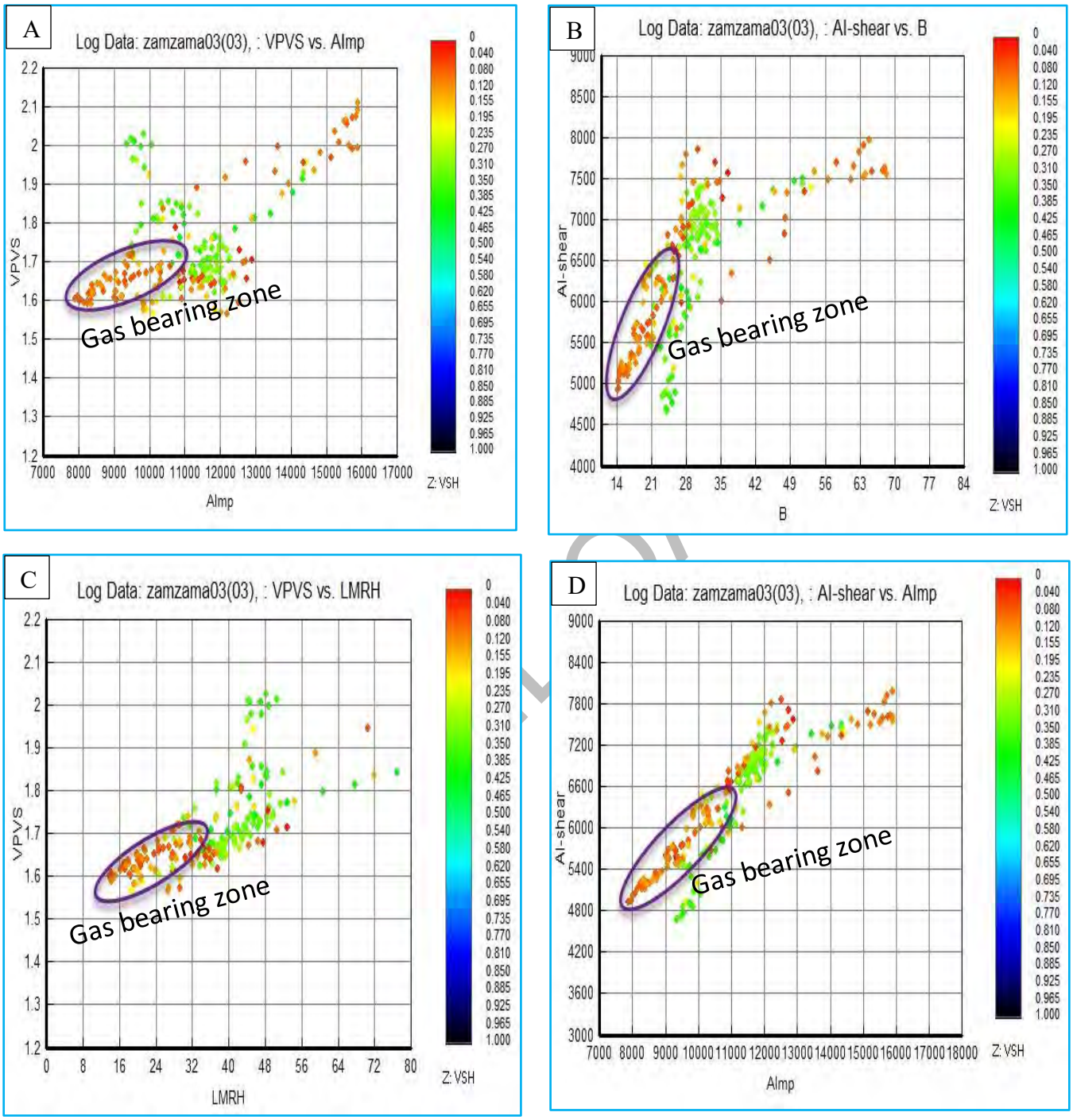

Figure 5.4: The crossplot analysis using Vsh at z – axis with marked gas bearing zone (A) v_p/v_s verses Aimp, (B) AI-shear verses bulk modulus, (C) v_p/v_s verses lamda row, and (D) AI-shear verses Aimp.

5.3.3 Crossplot analysis using Sw at Z-axis

The relationship between the Crossplot of Vp/Vs verses AImp, shear impedance verses bulk modulus, Vp/Vs ratio verses lambda row and shear impedance verses p-impedence is shown in Figure 5.5. In figure 5.5 four figures has been shown. In figure (a) a polygon is marked for the 1.5 to 1.8 range of the Vp/Vs ratio and low values of P-impedance, and SW(water saturation) provides colour labelling. A polygon is marked to indicate the values where the SW, P-impedance and Vp/Vs ratio all provide low values. SW is used for colour coding, as seen in figure (a).

Figure (b) shows shows crossplot of shear impedance verses bulk modulus. The marked polygon shows that shear impedance and P-impedence gives low values , SW22 is used for colour coding which predicts that marked zone is gas bearing zone.

Figure (c) depicts the crossplot of Vp/Vs ratio verses lambda row. The potential hydrocarbon zones must gives low values of Vp/Vs ratio and low to moderate value of lambda row which is marked by polygon as shown in figure (c).

Figure (d) gives the crossplot of shear impedance verses Aimp. For gas bearing zone shear impedance and P-impedence is always on lower side. Vsh is used for colour coding. The marked polygon in figure (d) completely depicts the gas bearing zone.

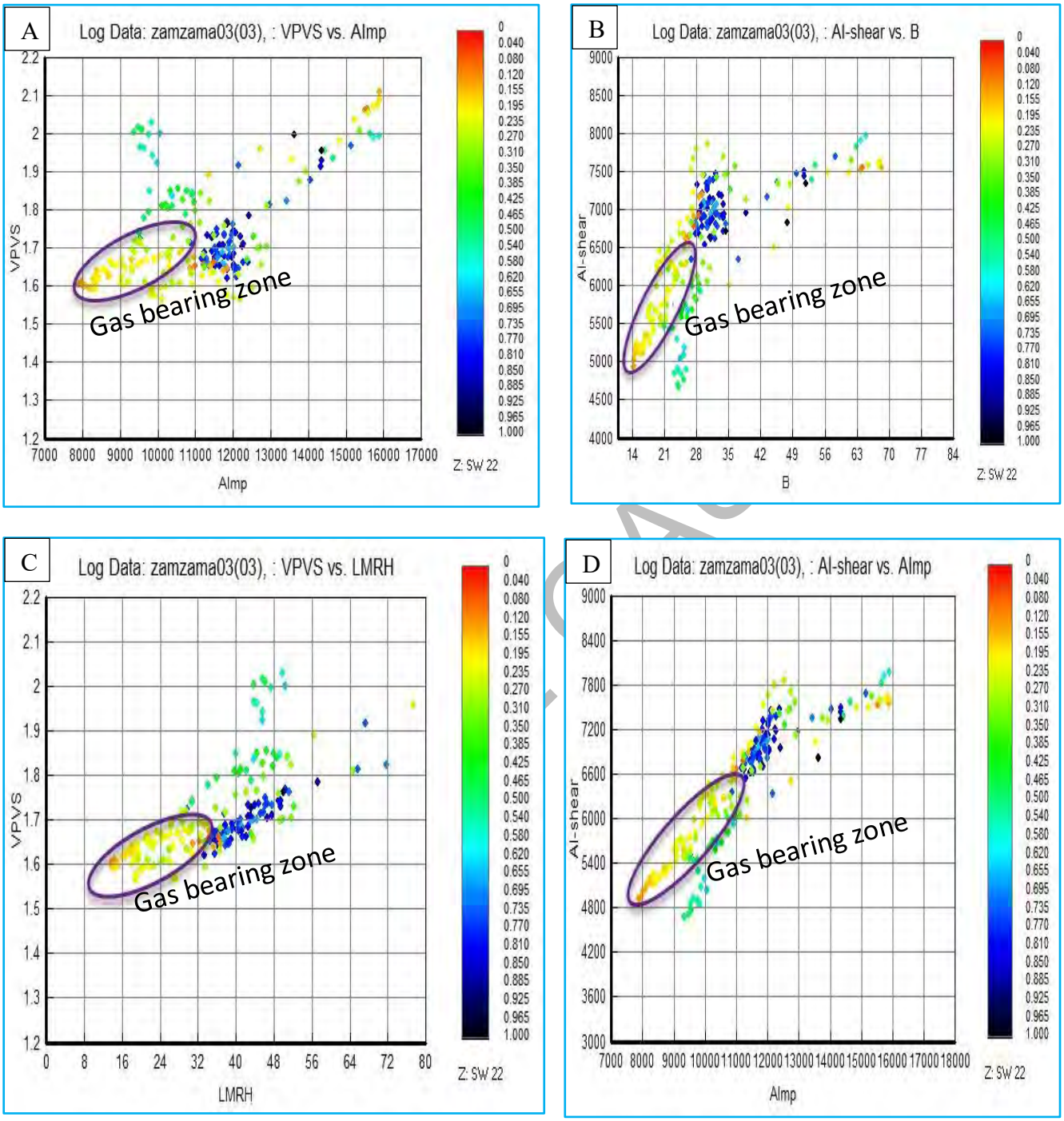

Figure 5.5: The crossplot analysis using Sw at z – axis with marked gas bearing zone (A) v_p/v_s verses Aimp, (B) AI-shear verses bulk modulus, (C) v_p/v_s verses lamda row, and (D) AI-shear verses Aimp.

CHAPTER#06

POST STACK INVERSION

6.1 Introduction

Because of its higher resilience and simpler assumptions, seismic post stack inversion is the most widely used technique. Broad band and Band Limited inversion are the two methods for post stack inversion, respectively (Russell, 2003). Model-based and Sparse Spike Inversion are other subtypes of broad band inversion.

Post stack Seismic inversion attributes are now commonly used to predict density, impedance and velocities ratio of P and S waves, also the elastic impedance from well log and seismic data. Exploration companies utilise the inversion approach to derive rock physical attributes from seismic data due to its effectiveness and increased quality. Construction of the first geological model precedes the use of real seismic data in inversion techniques. adjusted the model's parameters until the calculated and observed seismic data matched. Finally, matched geological model assistance for estimating reservoir physical property distribution. Recently, interest in seismic inversion has increased, and these integrated investigations are employed to explore for hydrocarbons . Seismic data can provide rich information on lithology and reservoir physical characteristics. Information from well logs can be directly related to seismic inversion, which converts interface property into stratigraphic property. This approach, geological interpretation from seismic data and inverted data, is useful for the characterization of reservoirs.

Several common seismic post-stack inversion techniques are employed for reservoir characterization, and the results are compared. On the post-stack seismic data of the Zamzama Gas Field, model-based (MBI), sparse-spike (SSI) (maximum likelihood), and band-limited (BLI) inversions are applied. The data is inverted into P-impedance and density volume in each case. High-resolution images between the time-depth ranges of 1700 and 2500ms are displayed in the final stacked segment. Within the target hydrocarbon sand, all inversions exhibit results that are mutually consistent and have low impedances. Every post-stack inversion technique yields precise, dependable findings and indisputably establishes the existence of a reservoir zone. Model-based inversion techniques have the lowest error and the highest correlation coefficient.

6.2 Methodology

The convolutional model is the foundation of seismic inversion. The earth's reflectance Rt is combined with the wavelet Wt and noise Nt, where * is the convolution operator.

$S_t = R_t * w_t + N_t$……...……6.1

In this case, St stands for the seismic trace, Rt for ground reflectance, Wt for a wavelet, and Nt for noise. If noise is assumed to be insignificant, equation 6.1 becomes,

$S_t = R_t * w_t$……...……6.2

Normal incidence earth reflectivity Rt is calculated by equation:

$R_t = \frac{\rho_j+1 v_j+1-\rho_j v_j}{\rho_j+1 v_j+1+\rho_j v_j}$……...……..6.3

Where, Zt=$\rho_j v_j$ is impedence, v_j is compression wave velocity, ρ_j is the density and layer j overlie on layer j+1.

Inversion is the process of estimating the inverse wavelet and combining it with seismic data to obtain the reflection coefficient. This is done by modifying equation (6.3), which calculates the impedance of each layer using equation (Russell, 2003).

$\rho_{j+1} v_j + 1 = \rho_j v_j \frac{1+R_j}{1-R_j}$……6.4

The equation above converts the layer attributes from the interface reflection coefficient.

6.3 Wavelet

It is not straightforward to create a synthetic trace using a wavelet convolve and reflectivity. The shape of a seismic wavelet changes over time and is quite complex. The various inversion techniques necessitate more precise wavelet prediction (Russell, 2003). The wavelet is not the same anywhere in the subsurface. Wavelet complexity is increased by the effects of the subsoil (geometrical spreading, attenuation) (Barclay et al., 2007). For this investigation, statistical wavelets are employed. The wavelength for statistical wavelet extraction is 200 ms, and the taper length is 25 ms. The time frame is between 2200 and 2400 ms. For synthetic purposes, zero-phase wavelets have been used. Figure 6.1 displays the extracted wavelet together with its amplitude and phase spectrum.

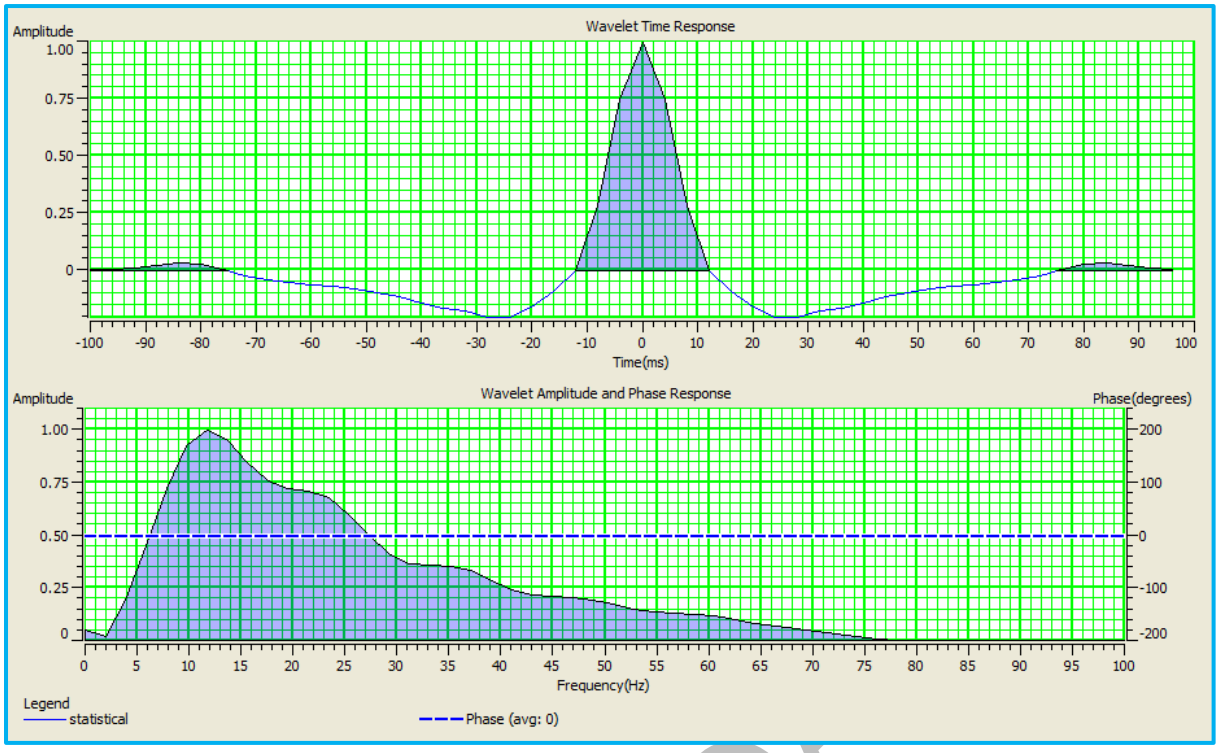

Figure 6.1:Extracted seismic statistical wavelet for seismic inversion analysis.

6.4 Low frequency model

There are two varieties of Acoustic Impedance: absolute and relative. As it is a relative feature of layers, "relative impedance does not need any starting lower frequency model for its computation" (Barclay et al, 2007). For qualitative seismic interpretation, relative impedance is employed. Cooke and Cant define absolute impedance as an absolute layer feature that affects seismic interpretation on both a qualitative and quantitative level (Cooke and Cant, 2010). Algorithms for inversion add frequencies to achieve absolute impedance (0–15 Hz) (Cooke and Cant, 2010). In model-based inversion, low frequencies constitute a component of the method, whereas in spare spike inversion, low frequency models are added independently (Cooke & Schneider, 1983). Figure 6.2 depicts the low-frequency inversion model used in this research. In this study, a sonic log is utilised to generate a low-frequency model near the wells.

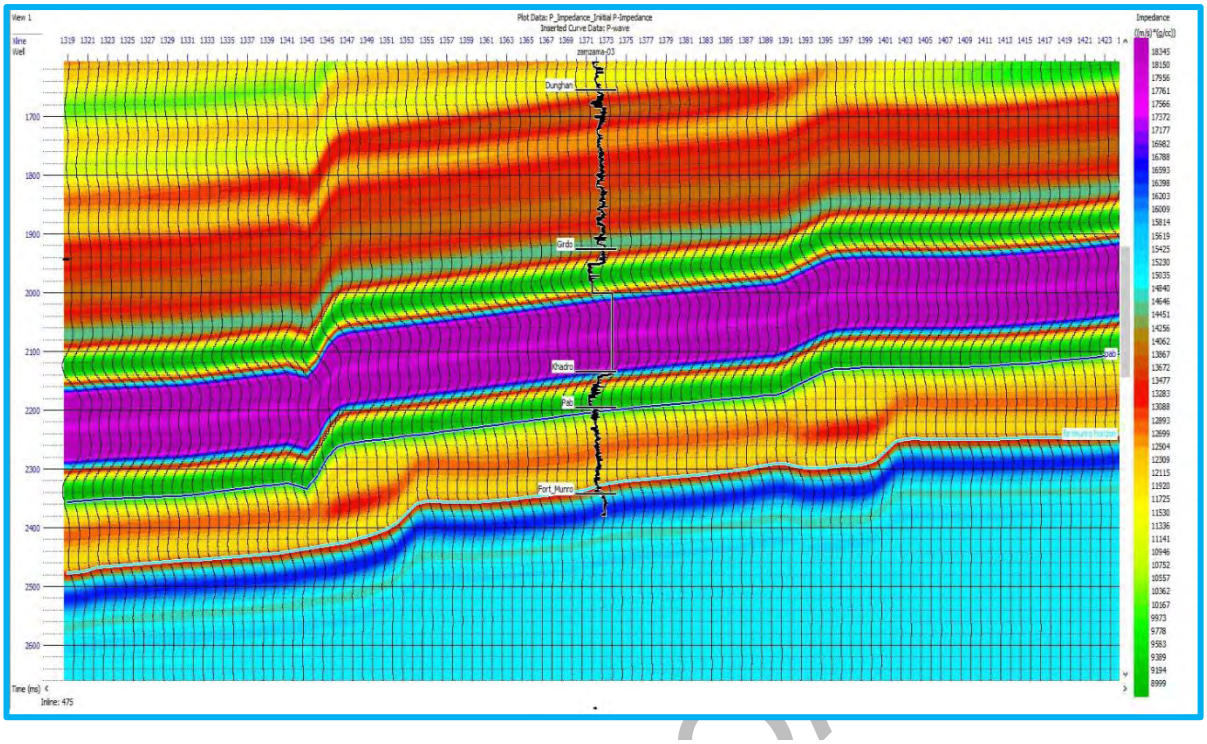

Figure 6.2:Low frequency model used for seismic model-based inversion algorithm.

6.5 Model based inversion

Logging constrained inversion based on convolution theory. According to the convolution theory, the source wavelet and ground reflectivity can be combined with noise to model the normal incidence seismic trace. A satisfactory correlation between a Synthetic Seismogram and a seismic trace is obtained by perturbing the initial geological model used in model-based inversion. Because it cannot directly invert seismic data, it is an appealing solution.

Because seismic data is band constrained and direct inversion methods cannot provide the precision and accuracy needed by the exploration sector, model-based inversion is effective for thin reservoirs.

Detailed information on stratigraphic and physical features is gained using model-based inversion, which has both high-frequency and low-frequency components.

$$J = Weight1 * (S_t - W * RC) + Weight2 * (M - P * RC) \quad \text{.....6.5}$$

where M is the initial guess model, St is the seismic trace, W is the extracted statistical wavelet, RC is the reflection coefficient, and P is the integration operator. These variables are convolved with the final reflectivity to generate the final impedance.

The seismic trace was modelled in the first part of the equation, and the predicted impedance was modelled in the second portion.

6.6 Inversion Analysis

Figure 6.3 displays the correlation between well log impedance and seismically determined Acoustic Impedance. The correlation coefficient between the seismic trace (red) and the synthetic produced from the well log (black) is 0.99854, with a 0.05 percent error. Inverted seismic impedance (red) picks up the trend of well log impedance (blue).

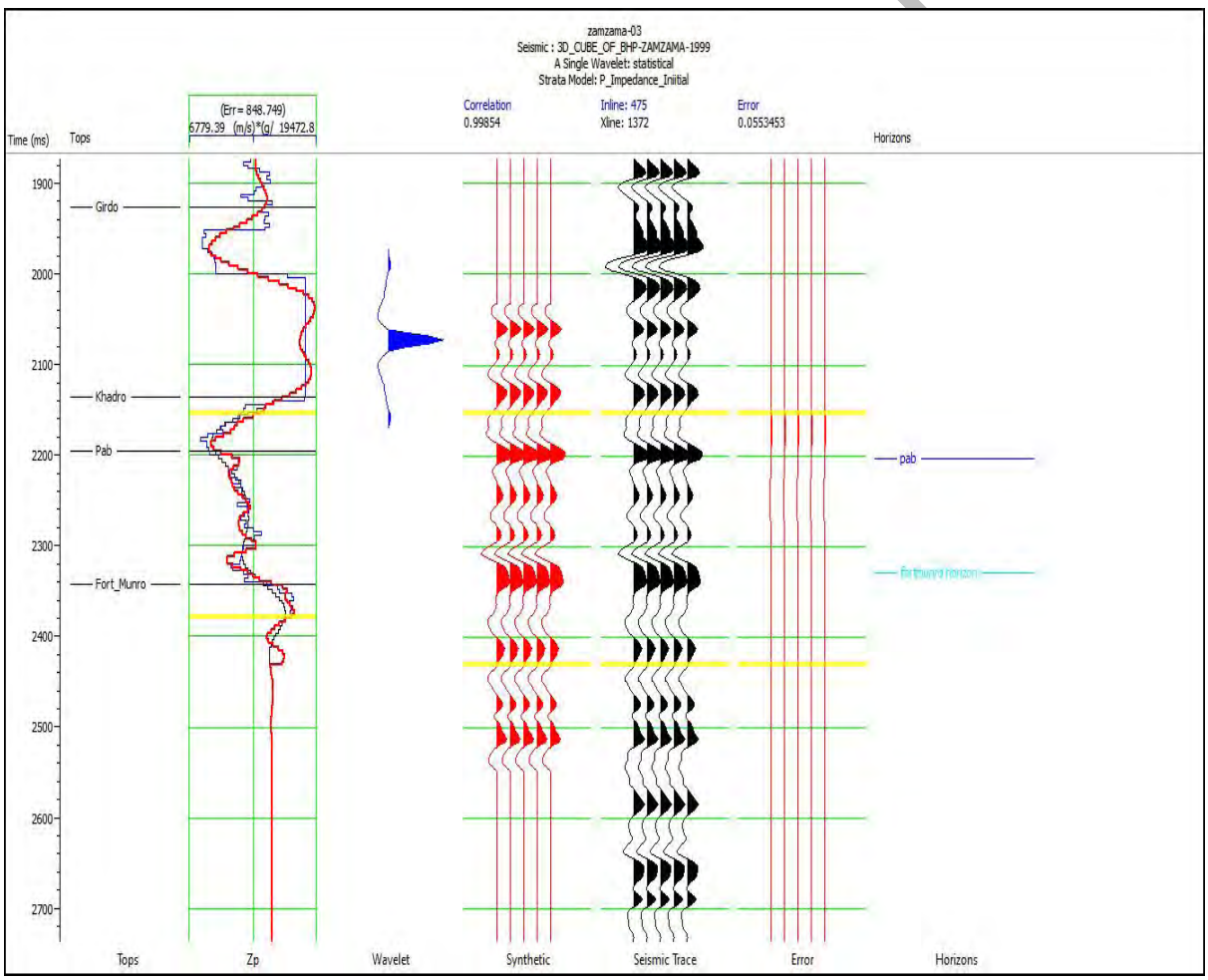

Figure 6.3:Inversion analysis results of model-based inversion with inverted impedance (red), log impedance (blue), low impedance model (black).

6.7 Inverted Section

Applying model-based inversion to the seismic region in Figure 6.4. The lateral and vertical fluctuations in Acoustic Impedance are captured by model-based inversion. The Low impedance in the Pab Sandstone, which begins at 2200 ms, is a sign of gas saturation and therefore is an area of interest.

The beginning of the Fort Munro Limestone marks the base of the Pab Sandstone, which has a high impedance. The model-based inversion has better vertical and lateral resolution and can detect impedance change within reservoirs.

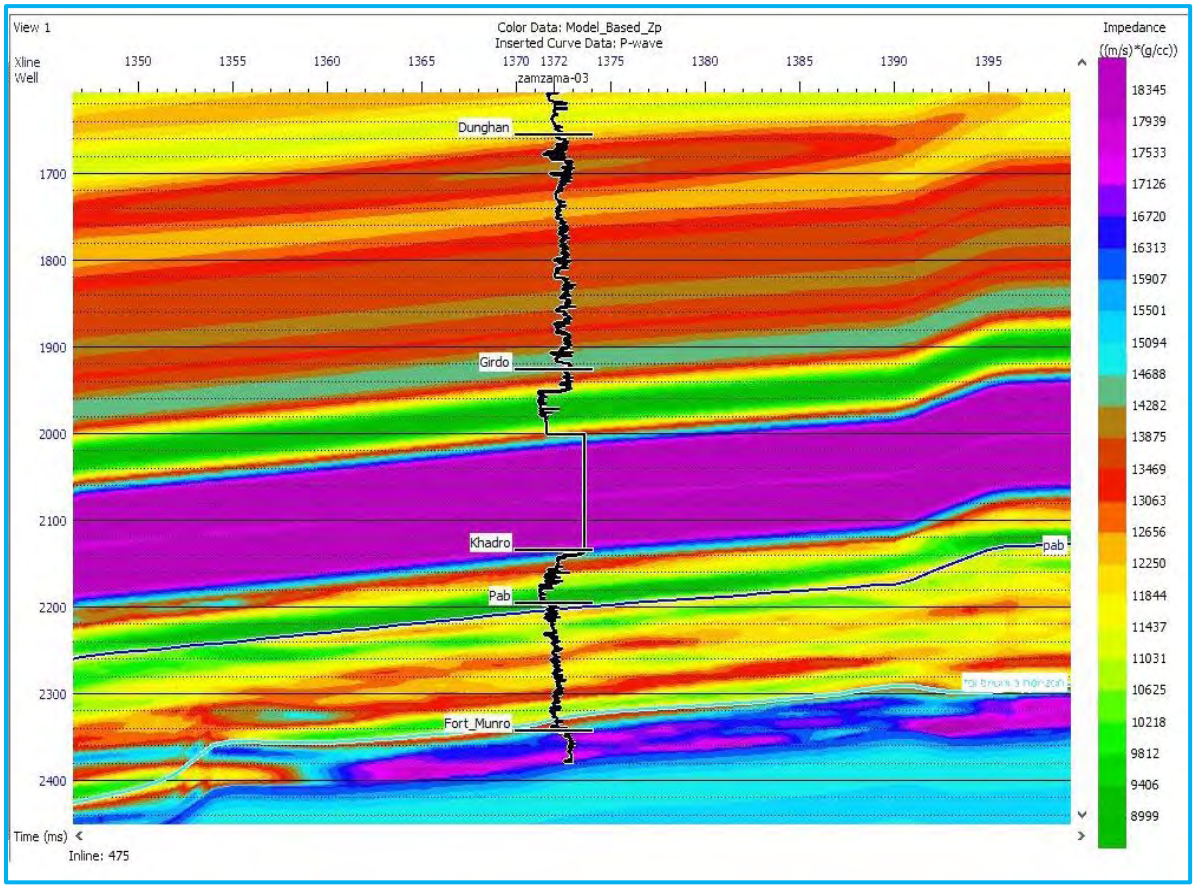

Figure 6.4:Inverted impedance of model-based inversion algorithm.

6.8 Sparse Spike Inversion

There are two ways to convert seismic section into impedance using Sparse Spike Inversion. These are maximum likelihood sparse spike and linear programming. The sparse spike algorithm perturbs a seismic data-derived reflectivity series using a model. The seismic data's wavelet is known.

When adding each reflection coefficient to a single trace, sparse reflectivity is produced until the desired set of outputs is reached. This form of reflectivity for a broad spectrum has gradually changed until the synthetic and actual traces are identical. Using the fundamental equation of the seismic trace, this technique uses the sparse reflection coefficient as the initial step in broad band seismic inversion.

$$S_t = R_t * w_t + N_t \quad \text{.....6.6}$$

Three unknowns are present in the equation above, and this approach makes wavelet approximations by assuming the reflectivity starting model. Sparse spike has an advantage over traditional deconvolution because it predicts the entire reflectivity bandwidth.

Maximum likelihood deconvolution inversion is the technique used. The objective function for method given as

$$J = \sum_{k=1}^{L} \frac{r2(k)}{R2} + \sum_{k=1}^{L} \frac{r2(k)}{R2} - 2m.\ln(\lambda) - (L-M).ln(1-\lambda) \quad \text{.....6.7}$$

where, $r2(k)$is reflection coefficient at kth sample is number of reflections, total number of samples is square root of noise variance is N and λ is likelihood of a given sample.

Lambda determines how many spikes should be anticipated. Our goal is to reduce the noise component and the number of spikes. By estimating the sparse reflectivity series and beginning with the initial wavelet applying further iterations until the objective function's low value is obtained.

When Sparse Spike Inversion is applied to the data, the well log impedance general trend is captured, but the resolution is higher than with band-limited inversion and lower than with model-based inversion.

According to Figure 6.5, the correlation coefficient between the inverted seismic trace (red), well logs (blue), and synthetic (black) is 0.970 with error 0.24 percent.

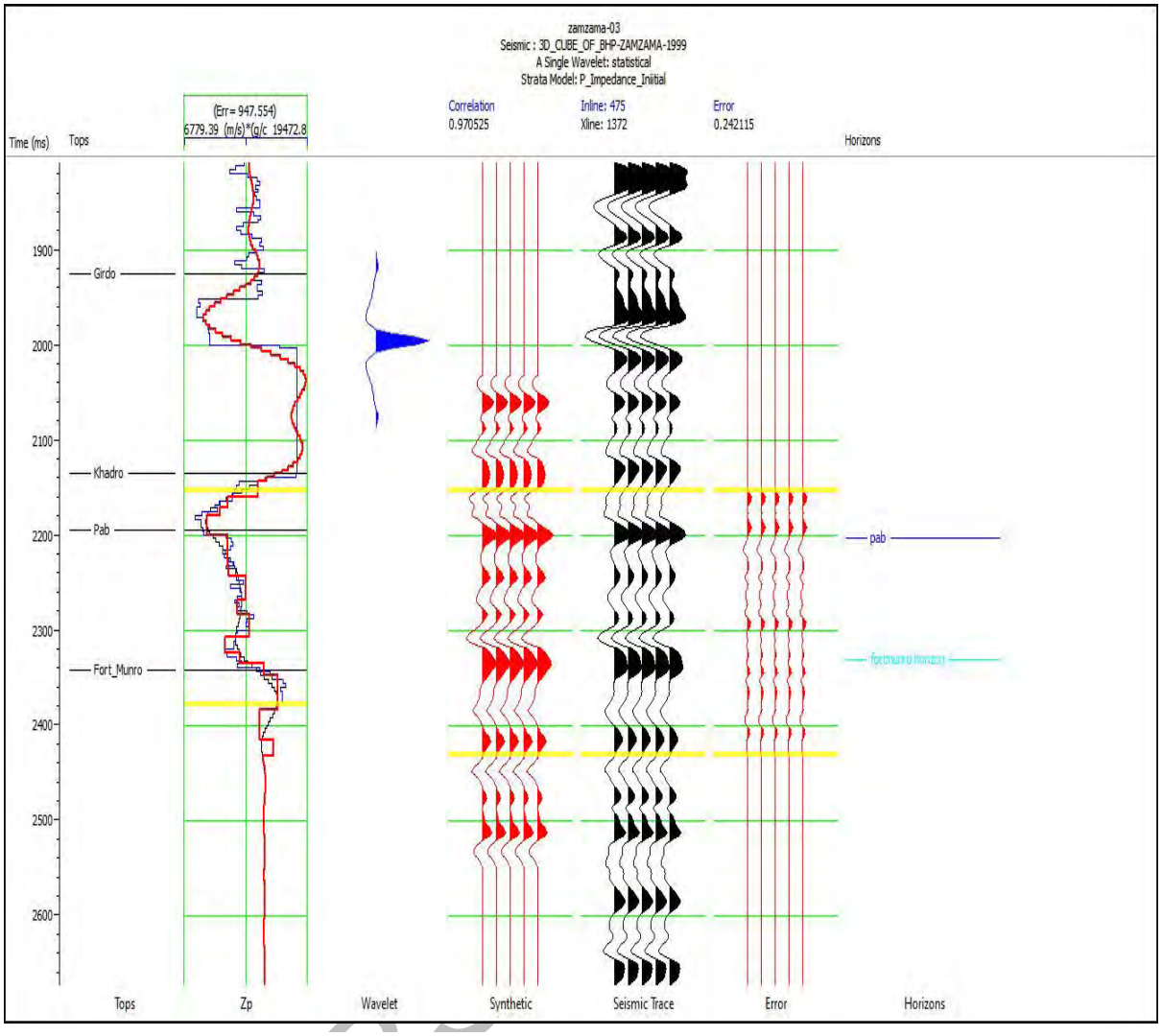

Figure 6.5:Sparse Spike Inversion analysis with inverted impedence(Red) and original impedence(Blue).

Figure 6.6 shows a Sparse Spike Inversion picking up the top of the Pab Sandstone. Fort Munro limestone has a high impedance (blue). Sparse Spike Inversion does not detect minor impedance variations in reservoirs and has a blocky impact and blurry pictorial representation.

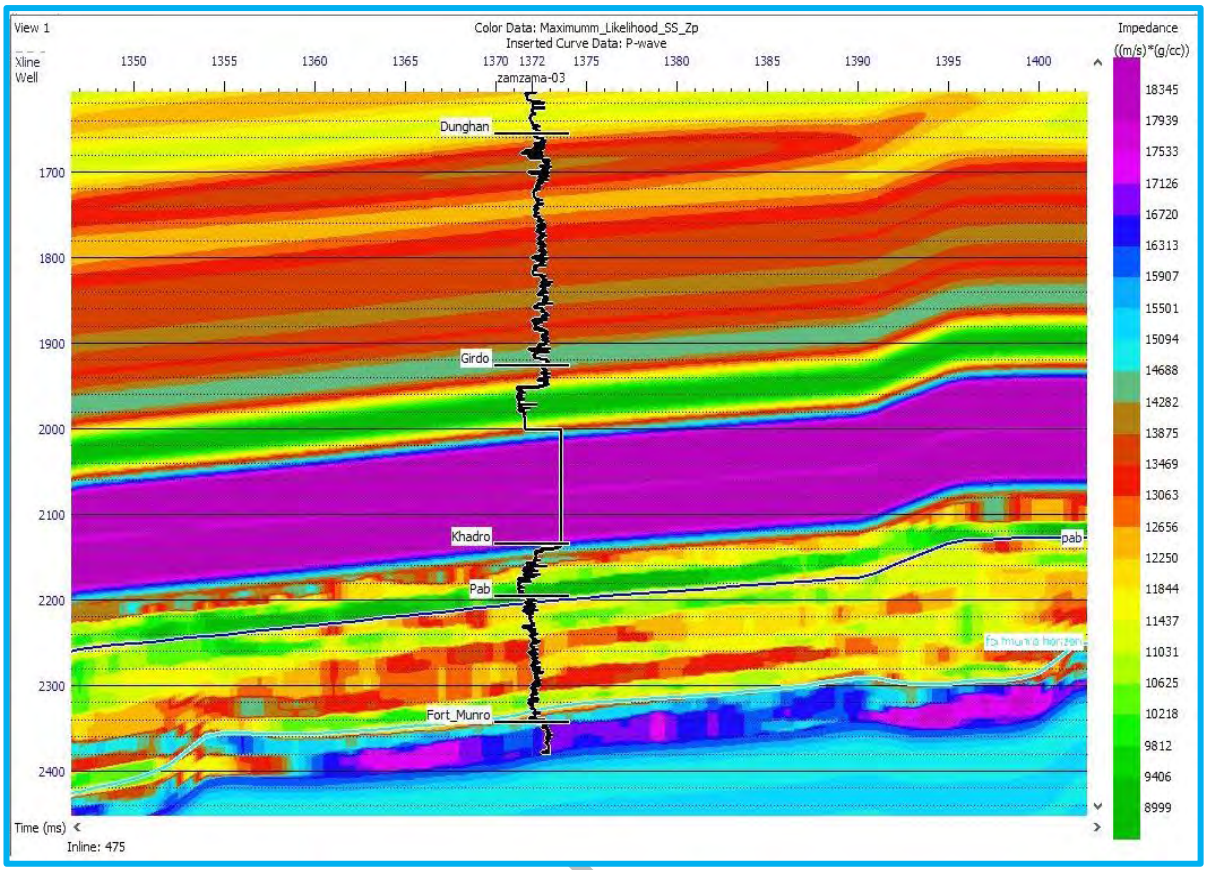

Figure 6.6.:shows Inverted impedance of Sparse Spike Inversion of Pab horizon.

6.9 Band Limited inversion(BLI):

Post-stack seismic data is converted into impedance, wave velocity, and density via band-limited inversion. Identifying the relationship between the seismic trace and impedance is the first step in band-limited inversion. Normal incidence reflection coefficient written as;

where, Z_i is seismic impedance of i layer and r_j is seismic reflectivity of i (i+1) layer.

$$\gamma_i = \frac{z_{i+1}-z_i}{z_{i+1}+z_i} \quad \text{.....6.8}$$

$$z_{i+1} = z_i \left(\frac{1+r_i}{1-\gamma_i}\right) \quad \text{.....6.9}$$

For n+1$^{th\ layer}$,impedence is given as,

$$z_n = z\left(\frac{1+\gamma_1}{1-r_1}\right)\left(\frac{1+\gamma_2}{1-\gamma_2}\right) \quad \text{.....6.10}$$

$$z_{n+1} = z_1 \pi_{k=1}^{j} \left(\frac{1+r_k}{1-\gamma_k}\right) \quad \text{.....6.11}$$

$$\ln\left(\frac{z_i+1}{z_i}\right) = \sum_{k=1}^{j} \ln\left(\frac{1+\gamma_k}{1-\gamma k} -\right) \approx 2\sum_{k=1}^{j} \gamma_k \quad \text{.....6.12}$$

$$Z_{i+1} = z_i Exp\left(2\Sigma_{k=1}^{j} rk\right) \quad \text{.....6.13}$$

$$S_k = \frac{2r_k}{\lambda} \quad \text{.....6.14}$$

Where, S_k is called reflectivity

Thus, equation (6.14) becomes,

$$Z_{i+1} = z_i Exp\left(\lambda\Sigma_{k=1}^{j} S_k\right) \quad \text{.....6.15}$$

We get the impedance trace by the integration of this equation.

6.10 Results of Band Limited inversion:

Seismic traces are subjected to band-limited inversion, and their impedance is calculated. Figure 6.7 displays the correlation coefficient, which is 0.954. The interpretation is resolved by the inverted impedance, which identifies faults and geological trends. Figure 6.8 shows the low impedance top of the Pab Sandstone, which was picked at 2200 ms.

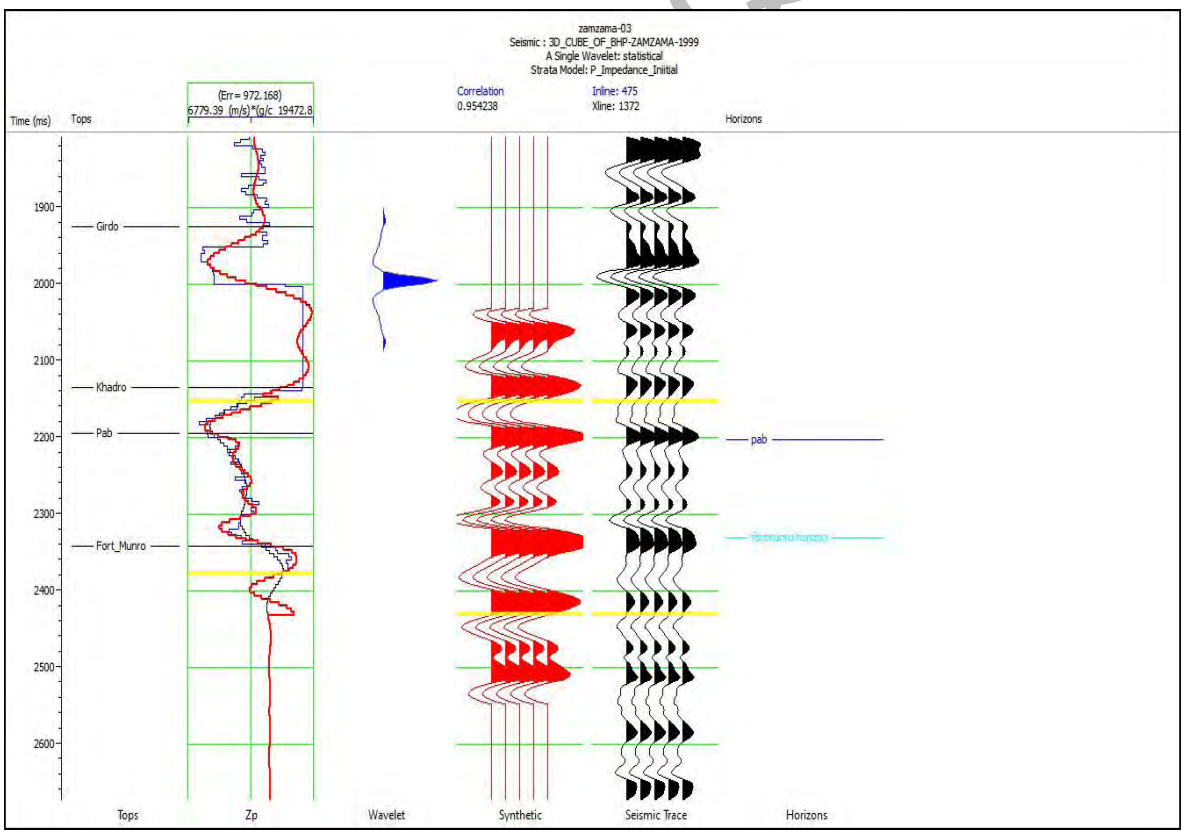

Figure 6.7:Band Limited Inversion analysis with inverted impedance (red) and original impedance (blue).

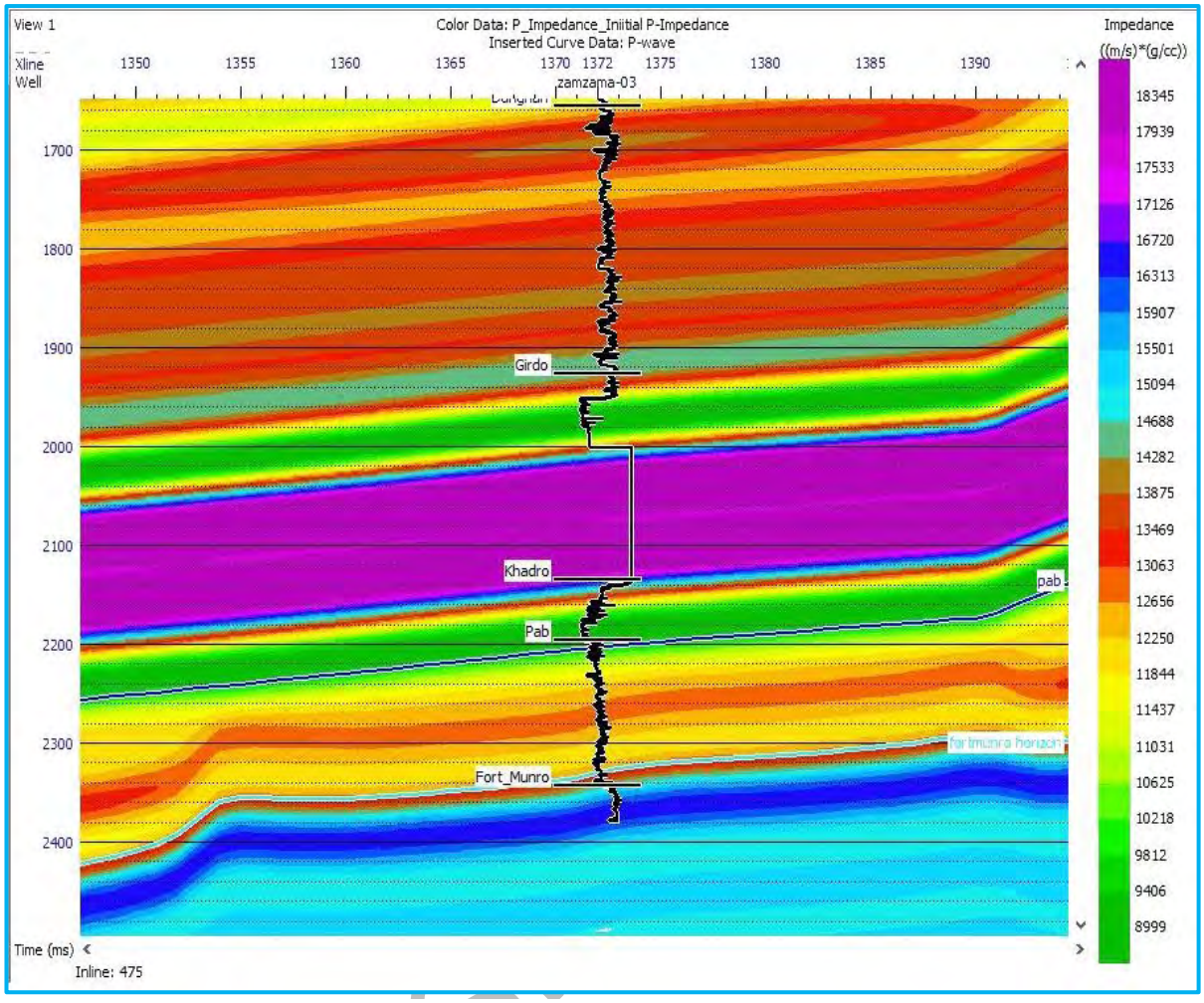

Figure 6.8.:Inverted impedance of Band Limited Inversion.

6.11 Comparison

For the impedance of Pab Sandstone in the Zamzama area, three post-stack inversion techniques—model-based, sparse spike, and band-limited inversion—have been employed, and the relative performance of each technique has been examined. All of the sections are solvable with inverted impedance from these three forms of inversions. However, inversion analysis When compared to sparse spike (0.970 correlation, 0.024 error) and band restricted (0.954 correlation), model-based inversion has a high correlation coefficient of 0.99 and less error of 0.05. The reservoir low impedance zone is resolved by each of the three inversion methods, as seen in Figure 6.9.

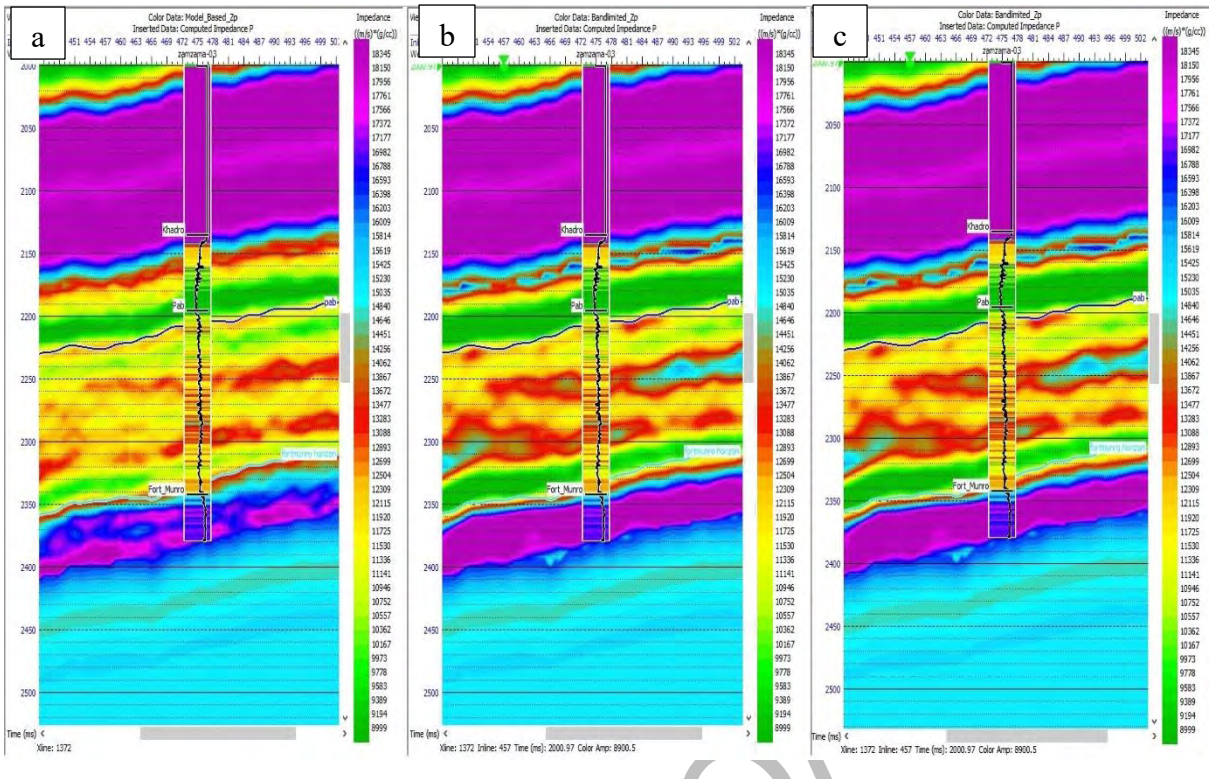

Figure 6.9:Comparative study of inverted impedance sections of MBI (a), BLI (b), and SSI (c).

Table 6.1 give the detail comparison of model based inversion, Sparse Spike Inversion, and Band Limited inverion on the basis of their impedance, correlation and estimated error.

Table 6.1:Comparison of model based, spasre spike, and Band Limited inverion on the basis of calculated values.

	Impedence	Corelation	Error
Model based inversion	9406-10000	0.99854	0.0553453
Sparse Spike Inversion	10000-11000	0.970525	0.242115
Bandlimited inversion	10600-11800	0.954238	

DISCUSSION AND CONCLUSION

This study's primary goals are to locate the gas sand reservoir and gauge its qualities. This assignment is carried out using 3D post stack seismic data from the Zamzama Gas field in the Lower Indus Basin, together with petrophysical and seismic interpretation and a comparative assessment of various post stack seismic inversion algorithms.

The procedure used to conduct this study is systematic in order to get the most information possible from the supplied data. The primary goal of the initial phase of the investigation is to best interpret the seismic section and identify the ideal structure for hydrocarbon formation. On the basis of reflector breaks and reflector dimming, two major faults are discovered and highlighted on seismic data, with faults F1 and F2 having a N-S orientation that leans toward the east. Two significant horizons, it is noted that the Fort Munro and Pab Formations are known late Cretaceous gas-dominated deposits. For the production of hydrocarbons, the Sembar formation serves as a source with a sizable volume of organic material. Although the water content in the Fort Munro limestone is high and makes extraction difficult, it does have the potential to deposit hydrocarbons such as gas. These two horizons are identified following the creation of a Synthetic Seismogram at Zamzama well 03 using a combination of sonic and density logs, as well as subsequent calculations of the Acoustic Impedance and reflection coefficient convolved with the extracted wavelet to produce a trace at the well location. This trace is then correlated with seismic at the well location to minimize interpretation error, a procedure known as seismic tie. Then, in order to break the contours and extend the fault across the entire area, we build fault polygons. For the purpose of providing lateral extension of Pab Formation, time and depth contour maps are constructed over the region. We can readily interpret these maps and recognise the structure based on colour variation. Average velocity is used on occasion when converting time to depth. Because it provides a solid foundation for seismic inversion, there should be very little room for interpretation mistake in this first section of the structural interpretation.

The interpretation of well log data is established in petrophysical analysis. Since well log data is collected so closely to the source, it has a very high resolution. The path to successful reservoir characterization is established by accurately handling the well log data. Lithology, resistivity, and porosity tracks, which are three fundamental and significant tracks, are used and Calculations are made to determine the zones that meet the criteria needed for a reservoir by taking into account the volume of shale (Vsh), porosities such as density porosity (PHID), total porosity (PHIT), and effective porosity (PHIE), as well as water saturation (Sw) and

hydrocarbon saturation (H.C). Zone1 having thickness (3700 –3720 m). In the Pab Sandstone one potential hydrocarbon-bearing zones, according to a petrophysical interpretation of the well Zamzama–03. Shale volumes in Zones1 average 21% and effective porosity is 10% with 24% average water saturation. The average hydrocarbon saturation is 76% . This zone is advantageous for exploring economically. A variety of inversion algorithms are used to accomplish post stack seismic inversion, Model based inversion (MBI), Sparse Spike Inversion (SSI), and Bandlimited inversion (BLI), three different forms of post stack seismic inversion techniques, are used to estimate reservoirs and analyze the results in inverted impedance maps. When comparing seismic and well log impedances, inversion analysis is used to determine the correlation coefficient and error. The difficult part was choosing an inversion technique that could precisely resolve Pab Sandstone. Using model-based inversion, low impedance zones are correctly identified with a correlation coefficient of (0.99) with error of (0.05). The correlation coefficient of maximum likelihood Sparse Spike Inversion is (0.97) with an error of (0.024), and Bandlimited inverted impedance also falls within acceptable ranges with a correlation coefficient of (0.95). When compared to SSI and BLI inversion techniques, MBI resolve the reservoir with the highest degree of correlation.

Rock physics gives the reasonable findings for reservoir zones, by calculating bulk modulus, shear modulus, possoin's ratio, Vp/Vs ratio, lambda row, meu row. All these parameters gives low values at reservoir zones. On the basis of these parameters and various crossplots two zones are marked as shown in figure 5.1.

Conclusions:

- The compressional regime of the research area's interpreted seismic section exhibits thrusted anticlinal structure, two reverse faults has been marked, which is further supported by time and depth contour maps.
- The Zamzama03 well's data shows that the Pab Sandstone reservoir having 10%PHIE, 24%Sw, and 70–80% hydrocarbon saturation, according to the results of the petrophysical analysis.
- Rock physics again conforms the reservoir zones by using different moduli parameters and by facies analysis of various crossplots of logs.
- Model based inversion (MBI), Sparse Spike Inversion (SSI), and Bandlimited inversion (BLI), three different forms of post stack seismic inversion techniques, are used to estimate reservoirs and analyze the results in inverted impedance maps.
- According to a comparison of inversion algorithms, MBI has more valid result than SSI and BLI in the studied area.

REFRENCES

- ASIM, S., BABLANI, S., QURESHI, S., & HUSSAIN, M. (2014). Seismic and well data interpretation for Fort Abbas area in Punjab Platform, Pakistan. *Sindh University Research Journal-SURJ (Science Series)*, *46*(3).
- Asquith, G., & Krygowski, D. (2004). AAPG Methods in Exploration, No. 16, Front Matter: Table of Contents, Acknowledgements, About the Authors, and Preface to First and Second Editions.
- Asquith, G. B., Krygowski, D., & Gibson, C. R. (2004). *Basic well log analysis* (Vol. 16). Tulsa: American Association of Petroleum Geologists.
- Bakker, P. M. (2002). Coupled anisotropic shear-wave ray tracing in situations where associated slowness sheets are almost tangent. *pure and applied geophysics*, *159*(7), 1403-1417.
- Coffeen, J. A. (1986). Seismic exploration fundamentals.
- Cosgrove, B. A., Lohmann, D., Mitchell, K. E., Houser, P. R., Wood, E. F., Schaake, J. C., ... & Meng, J. (2003). Real-time and retrospective forcing in the North American Land Data Assimilation System (NLDAS) project. *Journal of Geophysical Research: Atmospheres*, *108*(D22).
- England, R. W. (2004). BACON, M., SIMM, R. & REDSHAW, T. 2003. 3-D Seismic Interpretation. x+ 212 pp. Cambridge, New York, Melbourne: Cambridge University Press. Price£ 80.00 (hard covers). ISBN 0 521 79203 7. *Geological Magazine*, *141*(2), 245-246.
- Fischetti, A. I., & Andrade, A. (2002). Porosity images from well logs. *Journal of Petroleum Science and Engineering*, *36*(3-4), 149-158.
- Friend, P. F. (1998). BENDER, FK & RAZA, HA (eds) 1995. Geology of Pakistan. x+ 414 pp.+ maps in box. Beitrage zur Regionalen Geologie der Erde, Band 25. Berlin, Stuttgart: Gebrüder Borntraeger. Price DM 248.00, US $178.00 (hard covers). ISBN 3 443 11025 8. KAZMI, AH & JAN, MQ 1997. Geology and Tectonics of Pakistan. xiv+ 554 pp. Graphic Publishers, 5-c, 6/10 Nazimabad, Karachi, Pakistan. Price 1600.00 Pakistani rupees, US $34.00,£ 20.50 (hard covers). Order direct from publishers, adding US $12.00 for registered surface .... *Geological Magazine*, *135*(6), 819-842.

- Friend, P. F. (1998). BENDER, FK & RAZA, HA (eds) 1995. Geology of Pakistan. x+ 414 pp.+ maps in box. Beitrage zur Regionalen Geologie der Erde, Band 25. Berlin, Stuttgart: Gebrüder Borntraeger. Price DM 248.00, US $178.00 (hard covers). ISBN 3 443 11025 8. KAZMI, AH & JAN, MQ 1997. Geology and Tectonics of Pakistan. xiv+ 554 pp. Graphic Publishers, 5-c, 6/10 Nazimabad, Karachi, Pakistan. Price 1600.00 Pakistani rupees, US $34.00,£ 20.50 (hard covers). Order direct from publishers, adding US $12.00 for registered surface .... *Geological Magazine*, *135*(6), 819-842.

- Giroldi, L., & Alegria, F. (2005). Using spectral decomposition to identify and characterize glacial valleys and fluvial channels within the Carboniferous section in Bolivia. *The Leading Edge*, *24*(11), 1152-1159.
- Hussain, M., Ahmed, N., Chun, W. Y., Khalid, P., Mahmood, A., Ahmad, S. R., & Rasool, U. (2017). Reservoir characterization of basal sand zone of lower Goru Formation by petrophysical studies of geophysical logs. *Journal of the Geological Society of India*, *89*(3), 331-338.
- Kamel, M. H., & Mabrouk, W. M. (2002). An equation for estimating water saturation in clean formations utilizing resistivity and sonic logs: theory and application. *Journal of Petroleum Science and Engineering*, *36*(3-4), 159-168.
- Kazmi, A. H., & Jan, M. Q. (1997). Geology and Tectonics of Pakistan Graphic Publishers. *9789698375003*, *554*, 982.
- Kearey, P., & Brooks, M. (1988). Fundamentals of geophysics.
- Khan, A., & Connolly, J. A. D. (2008). Constraining the composition and thermal state of Mars from inversion of geophysical data. *Journal of Geophysical Research: Planets*, *113*(E7).
- Kushner, D. (1993). Sir George Darwin and a British school of geophysics. *Osiris*, *8*, 196-223.
- Olivier, G., Brenguier, F., Carey, R., Okubo, P., & Donaldson, C. (2019). Decrease in seismic velocity observed prior to the 2018 eruption of Kīlauea volcano with ambient seismic noise interferometry. *Geophysical Research Letters*, *46*(7), 3734-3744.
- Rajput, S., & Ring, M. (2014, March). The Role of Seismic Inversion in Exploration and Development: Adding Value and Reducing Uncertainties. In *Offshore Technology Conference-Asia*. OnePetro.
- Russell, B. H., Hedlin, K., Hilterman, F. J., & Lines, L. R. (2003). Fluid-property discrimination with AVO: A Biot-Gassmann perspective. *Geophysics*, *68*(1), 29-39.
- Phan, S. D., Gogoi, T., Chatterjee, R., & Sen, M. K. (2022). Predicting porosity, water saturation, and shale volume with high-resolution seismic inversion using Hopfield network: Upper Assam Basin, India. *AAPG Bulletin*, *106*(1), 103-118.
- Shamberger, K. E., Cohen, A. L., Golbuu, Y., McCorkle, D. C., Lentz, S. J., & Barklay, H. C. (2014). Diverse coral communities in naturally acidified waters of a Western Pacific reef. *Geophysical Research Letters*, *41*(2), 499-504.
- Shaw, R. K., & Sen, M. K. (2006). Use of AVOA data to estimate fluid indicator in a vertically fractured medium. *Geophysics*, *71*(3), C15-C24.
- Sroor, M. (2010). Geology and geophysics in oil exploration. *Mahmoud Ahmed Sroor*.
- Sturhahn, W., & Jackson, J. M. (2007). Geophysical applications of nuclear resonant spectroscopy. *SPECIAL PAPERS-GEOLOGICAL SOCIETY OF AMERICA*, *421*, 157.

- Symonds, G., Black, K. P., & Young, I. R. (1995). Wave-driven flow over shallow reefs. *Journal of Geophysical Research: Oceans*, *100*(C2), 2639-2648.
- Thompson, V. D., Reynolds, M. D., Haley, B., Jefferies, R., Johnson, J. K., & Humphries, L. (2004). The Sapelo Shell Ring complex: Shallow geophysics on a Georgia sea island. *Southeastern Archaeology*, 192-201.
- Trad, D., Ulrych, T., & Sacchi, M. (2003). Latest views of the sparse Radon transform. *Geophysics*, *68*(1), 386-399.
- Yielding, G., Badley, M. E., & Freeman, B. (1991). Seismic reflections from normal faults in the northern North Sea. *Geological Society, London, Special Publications*, *56*(1), 79-89.
- Zaigham, N. A., & Mallick, K. A. (2000). Prospect of hydrocarbon associated with fossil-rift structures of the southern Indus basin, Pakistan. *AAPG bulletin*, *84*(11), 1833-184
- Simm, R., Bacon, M., & Bacon, M. (2014). *Seismic amplitude: An interpreter's handbook*. Cambridge University Press.
- Avseth, P. A., & Odegaard, E. (2004). Well log and seismic data analysis using rock physics templates. *First break*, *22*(10).
- Jain, C. (2013). Effect of seismic wavelet phase on post stack inversion. In *10th Biann. Int. Conf. expo* (p. 410).
- Dar, Q. U., Pu, R., Baiyegunhi, C., Shabeer, G., Ali, R. I., Ashraf, U., ... & Mehmood, M. (2022). The impact of diagenesis on the reservoir quality of the early Cretaceous Lower Goru sandstones in the Lower Indus Basin, Pakistan. *Journal of Petroleum Exploration and Production Technology*, *12*(5), 1437-1452.
- Nazeer, A., Abbasi, S. A., & Solangi, S. H. (2016). Sedimentary facies interpretation of Gamma Ray (GR) log as basic well logs in Central and Lower Indus Basin of Pakistan. *Geodesy and Geodynamics*, *7*(6), 432-443.